HSN | University College of Southeast Norway

FMH606 Master's Thesis 2017

Energy and Environmental Technology

Microbial catalysis of syngas fermentation into biofuels precursors - An experimental approach

Pratap Jung Rai

Faculty of Technology, Natural sciences and Maritime Sciences

Campus Porsgrunn

University College of Southeast Norway

www.usn.no

Course: FMH606 Master's Thesis, 2017

Title: Microbial catalysis of syngas fermentation into biofuels precursors - An experimental approach

Number of pages: 61

Keywords: Fermentation; Syngas; Hydrogen consumption; Acetic acid and ethanol formation; Microbial synthesis; Acetyl-CoA pathway.

Student:	Pratap Jung Rai
Supervisor:	Carlos Dinamarca, Ph.D.
External partner:	
Availability:	Open

Approved for archiving: _____

(supervisor signature)

Summary:

Search for environment-friendly sustainable energy sources is of global interest due to continuous depletion of fossil fuels resources and excessive carbon dioxide emissions. Syngas fermentation is one of the promising sustainable alternative for liquid biofuel and chemical production from energy content wastes/byproducts. This study mainly focuses on acetic acid and ethanol production via fermentation, using hydrogen and carbon dioxide as substrates to mimic syngas. A laboratory scale, batch fermentation was performed at different headspace pressure ranged from 0.29 to 1.51 bar, 1200 rpm stirrer speed, and 22±1.4ºC.

Formation of acetic acid and ethanol were found significant. The maximum acetic acid concentration 68 mmol/L was obtained at 1176 hours and 1.12 bar headspace pressure. However, maximum ethanol concentration of 15 pA*s was found at 1297 hours and 1.51 bar headspace pressure. Ethanol consumption was observed during first 553 hours. Maximum H_2 consumption rate was 0.153 mmol/h·gVS during 478-527 hours at 1.12 bar headspace pressure, which was 51 times higher than that obtained during first 71 hours at 0.29 bar headspace pressure (0.003 mmol/h· gVS). The total consumed hydrogen gas measure as COD ($COD_{Hydrogen}$) was equivalent to the increase in bulk liquid COD, 11.02 gCOD and 11.44 gCOD; in which 68% of $COD_{Hydrogen}$ was converted to acetic acid (7.44 gCOD). A significant influence of headspace pressure and dissolved hydrogen concentration were observed on the volumetric mass (H_2) transfer coefficient (k_La) and the solubility of hydrogen in the inoculum (C_H). The maximum k_La and C_H of 0.082 h^{-1} ($R^2 = 0.995$) and 1.2 10^{-3} mol/L were found at 1.12 bar headspace pressure and 89 mmol/L dissolved hydrogen concentration, respectively. The calculated biomass yields ranged from 0.001-0.066 and 0.001-0.059 gVSS/gCOD, for acetic acid and ethanol formation, respectively, when the assumption of free energy efficiency use in growth was changed from 0.1 to 1.

Acetic acid and ethanol were dominant final product whereas other organic acids were almost constant and insignificant throughout the experiment. This implies that the microbial fermentation of hydrogen and carbon dioxide at headspace pressure ranged from 0.29-1.51 bar, 1200 rpm stirrer speed, and 22±1.4ºC, can be performed with digested food waste sludge for efficient acetic acid and ethanol production.

Preface

First of all, I would like to thank my supervisor, Assoc. Prof. Dr. Carlos Dinamarca for his invaluable support and guidance in accomplishing my thesis work and for being a motivating advisor to me both at USN and for my future career. I am also extremely thankful for all the effort and feedback during my bioreactor design and laboratory work.

I would also like to thank Dr. Eshetu Janka Wakjera, Hildegunn Hegna Haugen (Laboratory Manager), Fasil Ayelegn Tassew (Ph.D. student), Michal Sposo (Ph.D. student) and Khim Chhantyal (Ph.D. student) for offering their gracious help and time on research and laboratory work throughout my thesis period. I want to present my thanks to all the faculties of Technology at USN, Porsgrunn. I am equally grateful to University College of Southeast Norway (USN), Porsgrunn, Norway for the opportunity to study in this prestigious institution. In addition, I would express my gratitude to all my friends in Porsgrunn, Norway and Nepal for their continuous support and advice.

Finally, I am grateful to my Late father, Jivan Kumar Rai, he had faith in the struggle he flourished within me. I am also very thankful to my mother, Sita Rai, my sister, Shree Maya Rai, and my brothers, Pradeep Jung Rai and Pramod Jung Rai for their unconditional love and robust support throughout my life and for motivating me to never give up.

Porsgrunn, Norway, 15 May 2017

Pratap Jung Rai

List of abbreviations

Abbreviation	Description
Acetyl-CoA	Acetyl-coenzyme A
ACS	Acetyl-CoA synthase
ATP	Adenosine triphosphate
BWGS	Biological water gas shift
CODH	Carbon monoxide dehydrogenase
CODT	Total chemical oxygen demand
CODs	Soluble chemical oxygen demand
CSTR	Continuous stirred tank reactor
ETP	Electron transport phosphorylation
FBEB	Flavin based electron bifurcation
FDH	Formate dehydrogenase
Mo-CODH	Molybdopterin carbon monoxide dehydrogenase
Ni-CODH	Nickel-containing CODH
SLP	Substrate level phosphorylation
THF	Tetrahydrofolate
TS	Total solid
TSS	Total suspended solid
VFA	Volatile fatty acid
VS	Volatile solid
VSS	Volatile suspended solid
WLP	Wood Ljungdahl pathway

List of symbols

Symbol	Description	Unit
ε	Energy transfer efficiency	-
μ_{syn}	Specific growth rate of bacteria in microbial synthesis	$(\text{mol cell})^{-1}\text{h}^{-1}$
μ_{max}	Maximum specific bacteria growth rate	$(\text{mol cell})^{-1}\text{h}^{-1}$
C^*	Saturated dissolved gas concentration	mol/L
C_H	Solubility of hydrogen in liquid	mol/L
C_L	Measured gas concentration at the sampling time t	mol/L
C_S	Concentration of growth limiting substrate	mol/L
ΔG^{o}	Gibbs free energy	kJ/mole
ΔG_P	Free energy, convert carbon to pyruvate	kJ/e⁻eq
ΔG_{PC}	Free energy, carbon pyruvate to cellular carbon	kJ/e⁻eq
$K_{A,I}$	Undissociated acetic acid inhibition constant	mol/L
K_{CO_2}	Saturation concentration for carbon dioxide	mol/L
$K_{CO,I}$	Hydrogenase inhibition constant on CO	mol/L
k_{H,H_2}	Henry's coefficient for hydrogen	mol/atmL
$k_L a$	Volumetric mass transfer coefficient	h^{-1}
K_{H_2}	Saturation concentration for hydrogen	mol/L
P_{Gas}	Partial pressure of gas	bar or atm

Contents

List of figures

List of tables

1 Introduction

1.1 Introduction: necessities of syngas fermentation

Over the decades, the use of oil and fossil resources is being increased gradually. The increasing fuel demand diminishes the reserves of fossil fuel resources and creates the adverse impacts on the environment as a result of carbon dioxide emission [1]. Various renewable based energy technologies such as hydro, wind, and solar have already been developed and deployed to address the global energy demand. Although, oil and other fossil fuels still consider the primary source for energy demand and production. Therefore, it is an essential to go for alternative fuels to address these problems. The European Union has also instructed its member countries to use 10% of transport fuels should be derived from renewable-based sources, by 2020 [2].

Biofuels are considered as a sustainable alternative for non-renewable fossil fuels that offer very low CO_2 emissions [1, 3]. It can be derived through biochemical and thermochemical conversion processes [4, 5]. However, both conversion processes require specific condition, such as specific pretreatment; high temperature and pressure; low catalytic specificity and toxicity; and specific metal catalysts, to improve fermentation capacity for biofuels production [6-8]. Because the constraints faced in both conversion processes the need for alternative technology have been reinforced. Syngas fermentation is advocated as a promising alternative to produce biofuels and chemicals. Syngas, a primary mixture of hydrogen, carbon monoxide, and carbon dioxide, is the main component for subsequent biofuels and chemicals production [3]. In these days, important investments have been made for intensive research and development of syngas fermentation.

To obtain the experimental data for thesis dissertation, a laboratory-scale batch experiment was conducted to mimic syngas fermentation by using *hydrogen gas* and *sodium bicarbonate*, to analyze the microbial fermentation process. The pretreated food waste was used as an inoculum for fermentation, collected from two biogas industries, Porsgrunn, Norway.

1.2 Thesis objectives

The primary purpose of this master thesis is to understand the overall syngas fermentation process, focusing on mass transfer phenomena, bacterial consumption of the provided substrates and products distribution. In the experiment, *hydrogen gas* and *sodium bicarbonate* (in the bulk phase than balance with CO_2 depending on pH) are substrates and digested food waste is the inoculum used for acetic acid and ethanol production. The specific tasks given for master thesis are outlined as follows:

- Design, develop and test of laboratory scale batch fermentation bioreactor;
- Daily operation and sampling of the bioreactor;
- Experimental and literature data compilation and analysis;
- Identification of the most critical process parameters that affect the performance of syngas fermentation;

- Study and formulation of different stoichiometry reactions syngas fermentation that occur during syngas fermentation, along with kinetics of the process.

1.3 Report structure

The structure of thesis includes:

Chapter 2 gives a general literature review of syngas fermentation, along with microbial synthesis and acetyl-CoA pathway. The chapter also presents the most critical process parameters that hinder the microbial growth and microbial metabolism. Kinetics and stoichiometry of chemical reactions for bacteria growth are discussed.

Chapter 3 describes materials and methods which were used to expedite the experiments. Materials used for microbial fermentation are described; follow with details on design, installation, bioreactor test procedure, along with the experimental setup, procedure, and the performed experiments.

Chapter 4 includes the results extracted from the experiment, along with calculated biomass yields and stoichiometry of chemical reactions of the processes.

Chapter 5 presents the experimental results discussion about conflicting issues encountered in the previous chapter. This chapter also covers the discussion of calculated biomass yields and stoichiometry of chemical reactions of the process.

Chapter 6 covers the conclusions obtained from the discussions on Chapter 5 and the future works that are supposed to need further research and in-depth exploration.

2 Literature review

2.1 Syngas fermentation and microorganisms

2.1.1 Syngas fermentation as an alternate solution to biofuels production

Syngas fermentation is a microbial process, used to transform syngas into various sustainable biofuels and chemicals [9], that lowers not only the dependency on fossil fuels resources but also reduces greenhouse gas emissions [10]. Syngas fermentation offers several advantages compared to biochemical and thermochemical conversion processes (first and second generation processes) [5, 7, 11], such as high biocatalysts specificity; high toxic resistance; elimination of complicated pre-treatment steps and costly enzymes; lower energy costs; independence of $CO:H_2$ ratio; and higher carbon efficiency. Although it also has limitations that prevent it for commercialization, such as low productivity related to low cell density; high product recovery cost; slow reaction rates and product inhibition; and poor solubility of gaseous substrates in the liquid media [4]. Ethanol is the most useful product derived from syngas fermentation, uses as an additive to gasoline because of its high-energy content and high combustion efficiency. In practice, ethanol uses as a transportation fuel, blending with other fuels at different ratios (E10, E15, and E20) [12].

Figure 2.1 represents the schematic diagram of syngas fermentation process integrated with a biomass gasification.
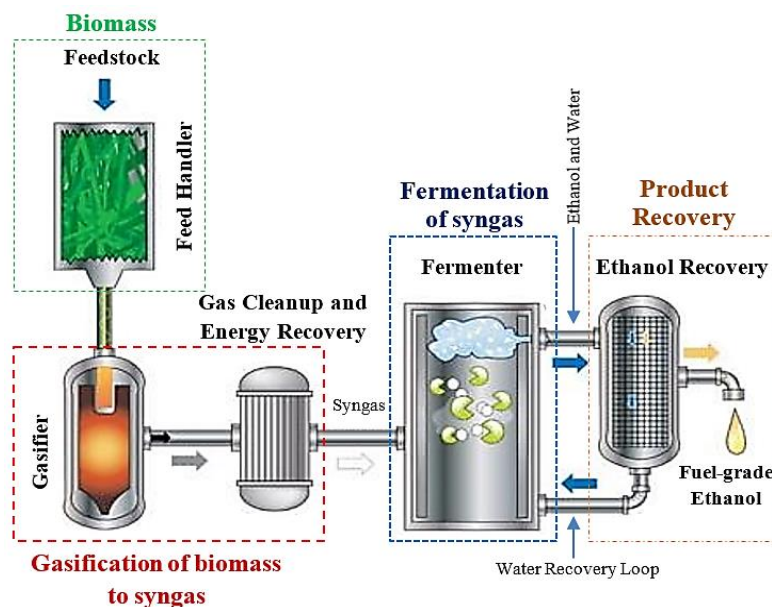
Figure 2.1: Process schematic diagram of syngas fermentation (source: www.coskata.com)

This process consists of feed handler, gasifier, energy recovery, fermenter and product recovery. A feed handler handles to deliver the biomass to the gasifier where biomass is

converted into gaseous fuels at temperature ranges between 750 to 900 ℃, under partial oxidation (less than 25% of the required amount of combustion) [13]. After gasification, the produced syngas passes through a gas clean-up unit to filter the unwanted products such as dust, ash, toxic components (discussed in Subsection. 2.3.7) and then energy recovery unit to recover heat via a heat exchanger. Then, clean compressed syngas is supplied to the fermenter that contained liquid media (food waste in our case), for fermentation. The fermenter is equipped with a stirrer that stirred continuously, to enhance the gas-liquid mass transfer. A mixture of biofuels and chemicals are generated that passed through a product recovery unit (distillation column), here where around 96 % ethanol is produced. The water is recycled back to the fermenter through a water recovery loop.

2.1.2 Syngas fermentation as an alternate solution to biofuels production

Several microorganisms (aerobic and anaerobic) involve in syngas fermentation that needs hydrogen, carbon dioxide, and carbon monoxide for building metabolic block [14]. Aerobic carboxydotrophic microorganism uses carbon dioxide as a sole carbon and energy source so that they can grow via molybdopterin carbon monoxide dehydrogenase (Mo-CODH) [15]. While, acetogen microorganisms such as *Acetobacterium woodii, Alkalibaculum bacchi, Clostridium ljungdahlii, Clostridium autoethanogenum and Clostridium thermoaceticum* are found in anaerobic nickel-containing CODH (Ni-CODH) enzymes and has 1000 times higher turnover number than the Mo-CODH [16]. Microorganisms capable of producing biofuels and biochemicals, with optimal temperature and pH are listed in Table 2.1. Generally, anaerobic acetogenic microorganism produces acetate, ethanol, butyrate, butanol and 2,3-butanediol and other valuable products.

2.2 Metabolic pathway and energy conservation

2.2.1 Biological water-gas shift reaction

Biological water gas shift (BWGS) reaction plays a significant role in fuel processing [17], in which water is mixed with CO in order to produce H_2 and CO_2. In BWGS, electrons and protons are extracted from CO oxidization due to the function of Ni-CODH enzymes in the anaerobic condition, shown in Reaction 2.1; protons are further reduced into hydrogen molecule by the CO tolerant hydrogenase enzymes, as seen in Reaction 2.2 [14].

$$0.5CO + 0.5H_2O \rightarrow 0.5CO_2 + H^+ + e^- \qquad \text{(R. 2.1)}$$

$$H^+ + e^- \rightarrow 0.5H_2 \qquad \text{(R. 2.2)}$$

$$0.5CO + 0.5H_2O \rightarrow 0.5CO_2 + 0.5H_2 \qquad \text{(R. 2.3)}$$

Reaction 2.3 represents the overall reaction of BWGS that derives the energy from the CO by transforming it into usable H_2 and CO_2, where hydrogen is liberated from the reactions and a partial amount of CO_2 converts into biomass and cell components

2.2.2 Reductive acetyl-CoA pathway

Reductive acetyl coenzyme A (CoA) pathway, also known as a Wood-Ljungdahl pathway (WLP), is one of the non-cyclic metabolic pathways discovered by Dr. Harold G. Wood and Dr. Lars G. Ljungdahl [18-20]. The autotrophic growth uses hydrogen as an electron donor, electrons extracted from H_2 oxidation, and carbon dioxide as electron acceptor derived from CO oxidation or The produced CO_2 is integrated into partial biomass cell component and partial remaining CO_2 reduction, to produce biofuels and chemicals [21, 22]. This metabolic pathway can be divided into two branches, namely methyl and carbonyl branch and they develop a single intermediate through the synthesis of CO and The produced CO_2 is integrated into partial biomass cell component and partial remaining CO_2, so-called reductive acetyl-CoA [23, 24], as shown in Figure 2.2 [24].

The methyl branch consists of 6 electron reduction steps of CO_2, where a number of sequential reduction reactions are to be involved in achieving methyl group of acetyl-CoA. According to the methyl branch sequence, the first step of transformation of CO_2 into formate is fulfilled by formate dehydrogenase (FDH) [20], which reacts with tetrahydrofolate (THF) and generates formyl-THF in adenosine triphosphate (ATP) consumption step. The generated formyl-THF converts into methyl-THF after subtracting a water molecule by the cyclohydrolase enzymes. Then, methyl-THF is reduced to methylene by a methylene-THF dehydrogenase [24]. A methyl group is then transferred to acetyl-CoA by combining CO molecule and CoA due to the action of bifunctional CODH/ACS enzyme [20].

The carbonyl branch consists of a single reduction reaction step whereas CODH plays a vital role to down CO_2 to CO to synthesize acetyl-CoA [24], as shown in Figure 2.2. But the conversion of CO_2 to CO faces a significant thermodynamic obstacle in acetyl-CoA pathway if CO is not available in fermentation media [22]. As described in Subsection 2.1.2, acetogens are able to produce acetate and ethanol. Therefore, as a key precursor, acetyl-CoA pathway is further treated to establish acetic acid and ethanol, in accordance with following overall stoichiometric reactions at 25 ℃ (Reaction 2.4 to 2.8) (Appendix A):

The stoichiometry for acetic acid formation.

$$4CO + 2H_2O \rightarrow CH_3COOH + 2CO_2 \qquad (\Delta G^o = \text{-157.36 kJ/mole}) \qquad (R.\ 2.4)$$

$$2CO_2 + 4H_2 \rightarrow CH_3COOH + 2H_2O \qquad (\Delta G^o = \text{-77.44 kJ/mole}) \qquad (R.\ 2.5)$$

The stoichiometry for ethanol formation.

$$6CO + 3H_2O \rightarrow C_2H_5OH + 4CO_2 \qquad (\Delta G^o = \text{-224.64 kJ/mole}) \qquad (R.\ 2.7)$$

$$2CO_2 + 6H_2 \rightarrow C_2H_5OH + 3H_2O \qquad (\Delta G^o = \text{-104.52 kJ/mole}) \qquad (R.\ 2.8)$$

It is clearly elucidated that CO is used as both sources (carbon and energy), to produce acetic acid and ethanol as shown in Reaction 2.4 and Reaction 2.7, respectively, or CO_2 as carbon source and H_2 as energy source used to obtain acetic acid and ethanol, shown in Reaction 2.5 and Reaction 2.7, respectively. However, CO utilization as both sources leads to low efficiency compared to CO as a carbon source and H_2 as an energy source.
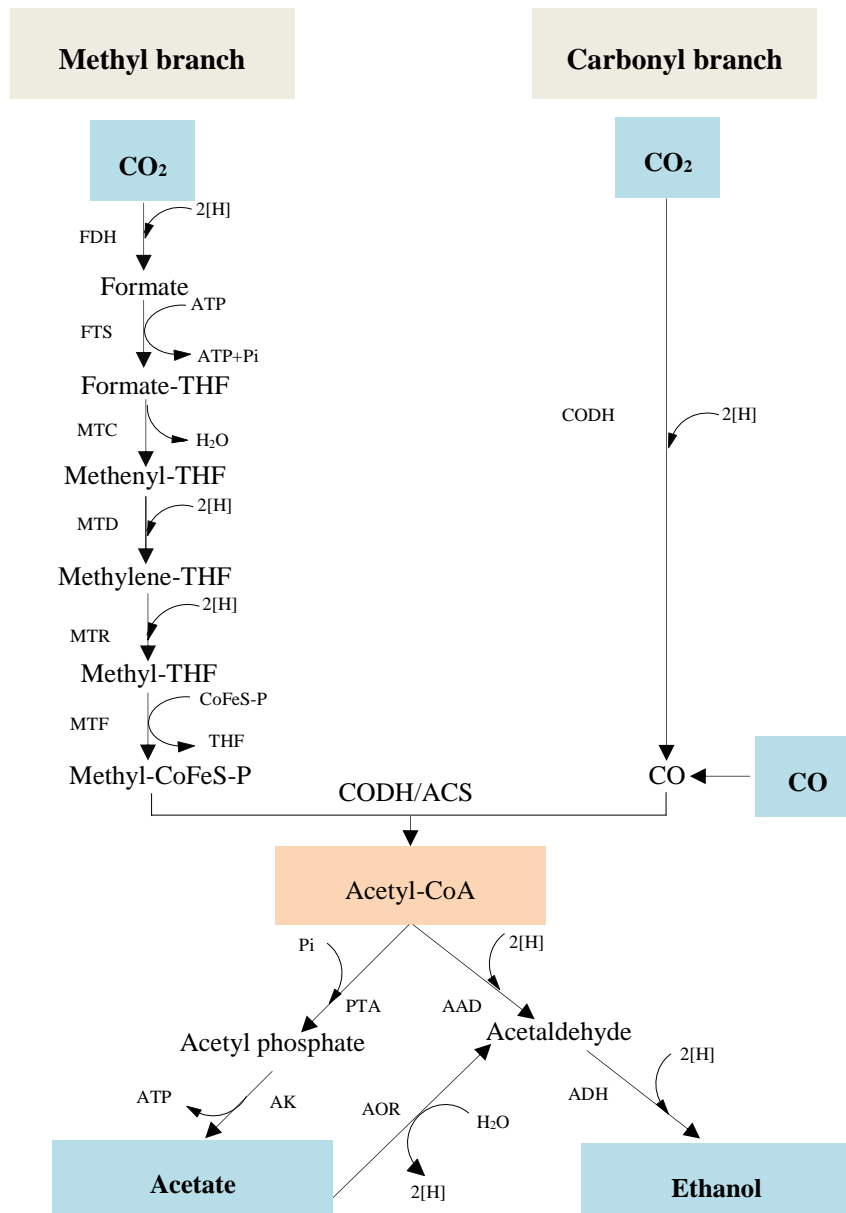
Figure 2.2: Reductive acetyl-CoA pathway overview of acetogenic bacteria [24].

ADH, aldehyde dehydrogenase; AOR, aldehyde oxidoreductase; CoFeS-P, corrinoid iron-sulphur protein; MTC, methenyl-THF; MID, methylene-THF; MIF, methyltransferase; MTR, methylene-THF.

2.2.3 Energy conservation in acetogens

The ATP is a convenient energy carrier where the acetyl-CoA pathway remains stable and conveys biochemical energy within cells, to support the metabolic processes. The acetyl-CoA pathway produces no net ATP through substrate level phosphorylation (SLP). The chemiosmotic ion gradient has been recognized as an important mechanism to drive ATP synthesis in autotrophic condition [25]. Few acetogens are an electron transport phosphorylation (ETP), are capable of functioning in anaerobic condition. The flavin-based electron bifurcation (FBEB) was found as an alternative means, for energy conservation [26]. FBEB sometimes combines not only with redox reactions but also clings to translocation of cations, so that creates the chemiosmotic gradient, as shown in Figure 2 [27]. According to the Latif et al. [27], Rnf complex consist of FBEB, are found in energy conservation enzymes that are capable of pushing H^+/Na^+ ion out from the cells. This could only happen when the oxidation of reduced ferredoxin combine with nicotinamide adenine dinucleotide (NAD^+) [28].
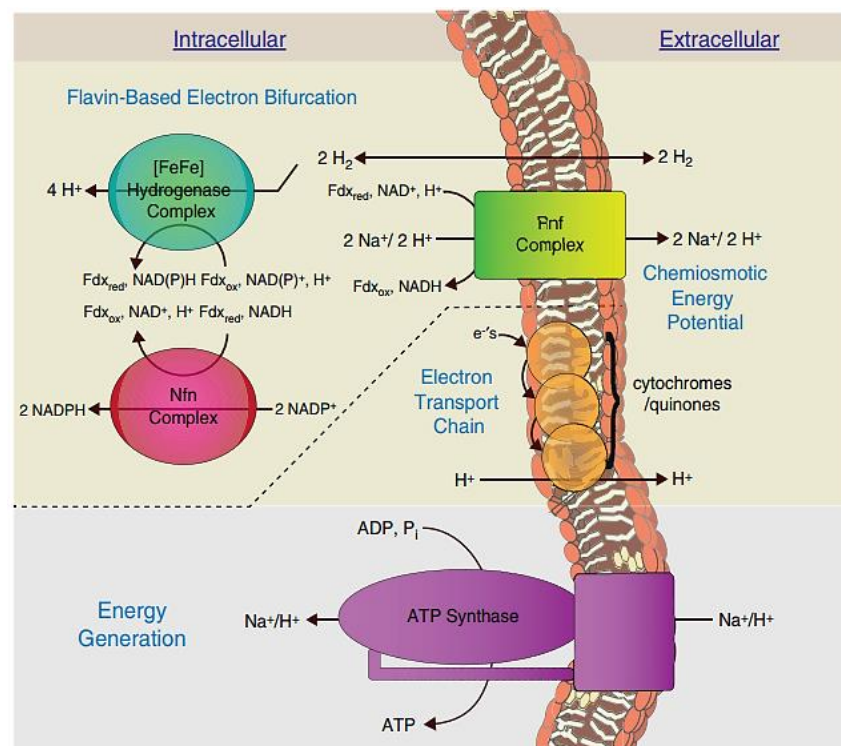
Figure 2.3: An overview of energy conservation during syngas fermentation [27].

Studies show that *Acetobacterium woodii* serves as a membrane-bound Na^+ dependent acetogens, generated from methyl-THF to CODH/ACS phase, for ATP synthesis [29]. On the other hand, *C. ljungdahliis* are unable to serve Na^+ translocating ATP ase. However, it creates H^+ translocating ATP ase, which is required to generate a proton gradient [30].

2.3 Syngas fermentation process parameters

2.3.1 Syngas partial pressure

Syngas partial pressure is one of the most important process parameters that plays the vital role in the microbial growth and fermentation efficiency. The gaseous substrates have low solubility in water; dense microorganisms face problems on the cell growth. Therefore, increase in partial pressure can overcome such problems by enhancing the mass transfer. In syngas fermentation, increase in partial pressure of CO (Pco), ranging from 0.35 to 2.0 atm, increases the cell concentration growth from 0.2 to 1.08 g/L [31]. Moreover, at high pressure, ranging from 1.35 and 2.0 atm, acetate consumption was noticed i.e. conversion of acetate into ethanol [31, 32]. This could be due to the onset of ethanol production by more utilization of electrons, occurring from CO oxidation [31]. Studies showed the concentration of ethanol yield and H_2/CO_2 was found high when total syngas pressure was high, between 1.6 and 1.8 atm. Since ethanol formation was high at high pressure, ethanol and acetate product ratio also found high at high pressure of 1.8 atm [33]. Furthermore, enzyme hydrogenase inhibition is another effect of increasing pressure of CO in the headspace. Kim et al. [34], performed an experiment on glucose content liquid media under the different headspace pressure of CO. The activity of hydrogenase (growth rate) was found decreasing at higher concentration of headspace CO. Study showed that approx. 90% of hydrogen uptake inhibition was observed at 0.084 atm of CO partial pressure [35].

2.3.2 Medium pH

Media pH has a strong influence on microbial catalysts and metabolic process. The optimum pH for microbial growth varies between 5.5 and 7.5, depending on the species used for syngas fermentation [32, 36]. An overview of optimal media pH for acetogenic microorganisms is given in Table 2.1. In an acetogenic microorganism (*e.g. Clostridium drakei, Clostridium autoethanogenum, Clostridium carboxidivorans P7 and Clostridium ragsdalei P11*), their metabolism is branched into two phases, acidogenesis or solventogenesis to produce acetic acid or ethanol, respectively [14]. The acetyl-CoA pathway tells that acidogenesis is associated with cell growth and equalized in ATP, but solventogenesis consumed ATP. That means, drop in pH leads to a reduction of cell growth and organic acid yield, that instigates to switch the fermentation phase from acidogenesis to solventogenesis [37]. The acetogen microorganisms are different from other microorganisms, which are unable to achieve constant media pH leading to an adverse effect on ethanol productivity. In order to overcome this problem, the multi-stage continuous system came up into use [38]. Switching of media pH by using multi-stage syngas fermentation would enhance biofuels production, where substrate metabolism is separated into acidogenesis and solventogenesis phase. For instance, the researcher examined two stage syngas fermentation process to improve ethanol productivity of Clostridium ljungdahlii, where the first stage maintained media pH of 5 and second stage, media pH of 4-4.5 [9]. Thirty times higher ethanol production was found while lowering pH in two stage continuous system compared to single continuous stirred tank reactor (CSTR) [38].

2.3.3 Fermentation temperature

Temperature is another most important process parameters in syngas fermentation that not only affects the microbial growth and substrate utilization, but also plays a significant role on the solubility of gaseous substrates. The most optimum temperature ranges for syngas fermentation microorganisms is found mesophilic, ranges between 37 and 40 ºC. While for thermophilic, optimum temperature ranges between 55 and 80 ºC. As temperature rises, chemical reaction and microbial growth get faster. However, high temperature may damage microorganisms growth and hinders the optimal biofuel conversion [39]. The thermophilic condition results lowering solubility of syngas (e.g. CO, CO_2, and H_2) and occurrence of contamination. Although, an increase in temperature enhances the mass transfer rate due to the low viscosity [11]. An overview of optimum temperatures of syngas microorganisms is given in Table 2.1.

Table 2.1: An overview of mesophilic and thermophilic microorganisms.

Species	T_{opt} (ºC)	pH_{opt}	Product(s)	Reference
Mesophilic microorganisms				
Acetobacterium woodii	30	7.0-7.2	Acetate	[40]
Clostridium aceticum	30	8.3	Acetate	[41]
Alkalibaculum bacchi	37	8.0-8.5	Acetate, ethanol	[42]
Butyribacterium methylotrophicum	37	5.5-7.4	Acetate, ethanol, n-butyrate, nbutanol	[43]
Clostridium autoethanogenum	37	5.8-6.0	Acetate, ethanol, lactate, 2,3-butanediol	[44]
Clostridium carboxidivorans P7	37	5.8-6.2	Acetate, ethanol, n-butyrate, n-butanol, lactate	[45]
Clostridium ljungdahlii	37	6.0	Acetate, ethanol, lactate, 2,3- butanediol	[3]
Clostridium ragsdalei P11	37	5.5-6.0	Acetate, ethanol, lactate, 2,3- butanediol	[46]
Thermophilic microorganisms				
Desulfotomaculum carboxydivorans	55	6.8-7.2	H_2, H_2S	[47]
Moorella thermoaceticum	55	6.8	Acetate	[48]
Moorella thermoautotrophicum	58	6.1	Acetate	[49]
Carboxydocella sporoproducens	60	6.8	H_2	[50]

2.3.4 Fermentation reactor design

Bioreactor design is identified as a crucial parameter for syngas fermentation, which has a close connection with mass transfer limitation. The bioreactor designer should address the following parameters, to achieve high productivity: high mass transfer rates, flexible to scale up reactor size, and low maintenance and operation cost. There are lots of bioreactors commonly used in practice, namely continuous stirred tank reactor (CSTR), bubble column reactor (BCR) and other bioreactors (e.g. trickle bed reactor, microbubble sparged reactors and packed bubble column reactors) [11, 14]. Among them, CSTR is one of the most common bioreactors, in which volumetric mass transfer coefficient can be enhanced by increasing feeding rate of syngas or increasing stirrer speed to improve the gas-liquid interfacial area [11]. In CSTR, syngas is continuously diffused into liquid media through the diffuser, at where large bubbles are broken down into the small bubbles by stirrer agitation. There are two methods to improve the volumetric mass transfer coefficient of gases substrates, one is a supply of feed at a high rate and another is an increase of gas-liquid interfacial area [14]. For instance, increase of CO specific flow rate from 0.14 to 0.86 vvm, corresponding with an increase of stirrer speed from 200 to 600 rpm, increases volumetric mass transfer coefficient of CO from 10.8 h^{-1} to 155 h^{-1} [51]. An overview of different types of bioreactors is given in Table 2.2.

Table 2.2: List of bioreactors used for syngas fermentation and volumetric mass transfer coefficient.

Bioreactor configuration	K_La (h^{-1})	Variables	Reference
Stirred tanks	10-500	Mixed speed, gas flow rate	[52]
Bubble columns	18-860	Gas flow rate, bubble size	[52]
Packed bubble column	18-430	Packing media, liquid flow rate, gas flow rate	[52]
Packed columns co-current flow	36-360	Packing media, liquid flow rate, gas flow rate	[52]
Microbubble sparged bubble column	200-1800	Size of bubble	[53]
Internal loop airlift	140-220	Aeration rate, liquid flow rate	[54]
Airlift reactor with a net draft tube	18-160	Air velocity, pressure of reactor	[55]

2.3.5 Medium formulation

Media formulation plays a significant role in determining desired products and species in syngas fermentation [11]. To achieve maximal metabolic activity and microbial growth, bacteria needs different constituents in the media, such as vitamins, mineral nutrients, calcium pantothenate, and cobalt [21, 56], including yeast extract as nitrogenous compounds [57].

Replacing expensive media nutrient by cheap organic media reduces fermentation medium cost and enhances the overall cost of processes. Studies showed that the media without yeast extract is found in residing *C. ljungdahlii* cultures with limited metabolic activity and biochemical concentrate [58, 59]. However, inadequacy amount of nutrient creates metabolic shift (solventogenesis), it may cause a reduction in cell viability and product formation. Thus, at least small amount of yeast extract as a nutrient is required to improve product formation. However, yeast extract is an expensive media. Therefore, it would be better to replace with cheap media such as steep corn liquor for *C. ragsdalei P11* and cotton seed extract for *C. carboxidivorans P7*. The results showed 60% improvement in ethanol production [60].

2.3.6 Rate limiting factor

There are two rate limiting steps, namely kinetic-growth limitation and mass transfer limitation that play a crucial role to optimize the productivity of biofuels and chemicals [57]. Kinetic-growth limitation basically appears in low cell density and low metabolic activity fermentation, such that substrate concentration in the liquid phase is comparatively high due to the low substrate consumption rate. In contrast, gas-to-liquid mass transfer limitation is found in high cell density and metabolic activity fermentation. It has severe impacts on biofuels and chemicals production due to the resistance of gaseous substrate diffusion [7]. Because of diffusion limitation in the fermentation liquid media, microorganisms consume a low amount of substrate that causes low in products production [11]. Therefore, it is necessary to address the issues raised by mass transfer limitation, which can be determined by using following Equation 2.1.

$$\frac{dC_L}{dt} = k_L a (C^* - C_L) \qquad\qquad\qquad \text{(Eq. 2.1)}$$

where $k_L a$ is the volumetric mass transfer coefficient, C^* is the saturated dissolved gas concentration, and C_L is the measured/dissolved gas concentration at the sampling time t. As discussed in above subsection, the volumetric mass transfer coefficient ($k_L a$) can be enhanced either by increasing impeller speed or by increasing gas flow rate. Increasing agitation speed increases the breakup of bubbles developed from gases diffusion, which increases the interfacial area for mass transfer [32]. However, increasing agitation speed is not always economically feasible to improve $k_L a$ due to extra power requirement and sometimes high agitation speed harms some sensitive bacteria, whereas increasing gas flow rate also causes gases substrates wastage. An experiment performed by Bredwell and Worden, [53] showed that initiating micro-bubble spreading in liquid media the $k_L a$ for CO increased by six times. Similarly, increase in gas flow rate in CSRT within cell kinetic requirement resulted in a higher CO conversion. But, if the gas flow rate is beyond cell kinetic requirement, conversion efficiency keeps constant [61]. Table 2.2 provides the $k_L a$ of different bioreactors.

2.3.7 Syngas composition

Syngas consists of a different ratio of gases such as H_2, CO and CO_2 (primary components) [62] and other impurities (e.g., N_2, NH_3, HCN, O2, SO_2, Nox, tars, ash, and H_2S if they are extracted from gasified biomass) [11]. These impurities have a strong influence on syngas fermentation. Bacteria can use CO as a sole source of energy and carbon, for biofuel production. However, CO inhibits the hydrogenase. Therefore, a significant amount of hydrogen should be presented in syngas fermentation, to optimize the biofuel production [21]. Syngas consists of impurities that cause low cell growth, cell dormancy, hydrogen uptake restriction, including metabolic shift between acidogenesis and solventogenesis [62]. For instance, nitrogen content syngas converts into NH_3, HCN, and NOx in the culture medium that causes inhibition of biocatalysts function, in where high NH_3 accumulation hinders cell growth of acetogen significantly. Similarly, tar in the gas substrate causes cell dormancy and disturbance in acetic acid/ethanol product distribution [63]. To improve biofuels production, an appropriate method should be used to avoid impurities content in the syngas. The source of impurities is depended on the type of feedstock, operating condition, and type of gasifier.

2.4 Microbial kinetics of syngas fermentation

The mass of the active biomass and gas substrate should be balanced in the microbial process, to determine the biomass growth and substrate utilization. Monod equation, Equation 2.2 is used to express bacterial growth kinetics, [64].

$$\mu_{syn} = \mu_{\max} \frac{C_S}{K + C_S} \qquad\qquad \text{(Eq. 2.2)}$$

where μ_{syn} is the specific bacteria growth rate, $\mu_{\max}$ is the maximum specific bacteria growth rate, K is the half saturation constant, substrate concentration giving one-half the maximum rate, and C_s is the concentration of growth limiting substrate. Biomass and gaseous substrates may contain inhibitory compounds, which may create obstacles on microbial growth rate and substrate utilization. Because of it, biofuels and chemicals formation reduction could be encountered. Bacteria requires energy for both growth and maintenance that only can obtain from oxidation-reduction reactions. Thus, bacteria growth involves the biological reactions for energy production and cell synthesis.

Equation 2.3 and Equation 2.4 represent kinetic expression for specific cell yields and acetic acid production from hydrogen and carbon dioxide, respectively. In this expression, two Monod kinetics were used to express the both gaseous substrates limitation, accompanied with hydrogenase inhibition due to carbon monoxide and product inhibition by undissociated acetic acid.

$$\mu_{yield,1} = \mu_{max,1} \frac{C_{H_2}}{K_{H_2} + C_{H_2}} \frac{Cco_2}{Kco_2 + Cco_2} \frac{K_{CO,I}}{K_{CO,I} + Cco} \frac{K_{A,I}}{K_{A,I} + C_A} \qquad \text{(Eq. 2.3)}$$

$$\mu_{acetic\ acid} = \mu_{max,2} \frac{C_{H_2}}{K_{H_2} + C_{H_2}} \frac{Cco_2}{Kco_2 + Cco_2} \frac{K_{CO,I}}{K_{CO,I} + Cco} \frac{C_{A,I}}{K_{A,I} + C_A} \qquad \text{(Eq. 2.4)}$$

where K_{H_2} and Kco_2 are the saturation concentration of hydrogen and carbon dioxide, respectively. The parameter $K_{CO,I}$ is carbon monoxide inhibition constant on hydrogenase, when there is no CO present (CO< $K_{CO,I}$), the growth will not be inhibited. The parameter $K_{A,I}$ is unbroken acetic acid inhibition constant for H_2 and CO_2 [32].

Equation 2.5 and Equation 2.6 describe kinetic expression for biomass growth and ethanol production on hydrogen and carbon dioxide, respectively. Although, it is only workable if carbon monoxide concentration is very low than hydrogenase inhibition constant.

$$\mu_{yield,2} = \mu_{max,3} \frac{C_{H_2}}{K_{H_2} + C_{H_2}} \frac{Cco_2}{Kco_2 + Cco_2} \frac{K_{CO,I}}{K_{CO,I} + Cco} \frac{K_{A,I}}{K_{A,I} + C_A} \qquad \text{(Eq. 2.5)}$$

$$\mu_{ethanol} = \mu_{max,4} \frac{C_{H_2}}{K_{H_2} + C_{H_2}} \frac{Cco_2}{Kco_2 + Cco_2} \frac{K_{CO,I}}{K_{CO,I} + Cco} \frac{C_{A,I}}{K_{A,I} + C_A} \qquad \text{(Eq. 2.6)}$$

If there is no carbon monoxide, growth will not be inhibited. But, if there is CO that reduces the specific cells growth because of hydrogenase inhibition. Therefore, carbon monoxide will be consumed initially and then shift towards other gaseous substrates, to produce acetic acid. The continual cells growth, biofuels, and chemicals will limit because of undissociated acetic acid accumulation on hydrogen and carbon dioxide fermentation.

2.5 Conclusions

Syngas fermentation (gas to liquid technology) has become an emerging sustainable solution for biofuels and chemicals production. The production of chemicals and biofuels via syngas bioconversion, extracted from agricultural waste, non-food energy crops, and waste gases can be an alternative solution for energy demand and greenhouse emission reduction. Although, it seems challenging the production of chemicals and biofuels in an effective way due to too many parameters and limitations that need to be controlled. Section 2.3 clearly describes that there are several parameters, such as partial pressure, media pH, temperature, bioreactor design, medium formulation, rate limiting factor, and gas composition, they severely affect the productivity of fermentation. However, there are also many advantages of syngas fermentation, one of them is that is capable of capturing industrial waste gases and convert them into valuable chemicals and biofuels.

3 Materials and Methods

3.1 Materials: inoculum

The digested food waste sludge was used as the liquid media (i.e. inoculum), collected from biogas plants (*Hadeland og Ringerike Avfallsselskap* and *Indre Agder og Telemark Avfallsselskap IKS*), Porsgrunn, Norway. A series of treatments were performed to achieve required inoculum properties, as shown in Figure 3.1.
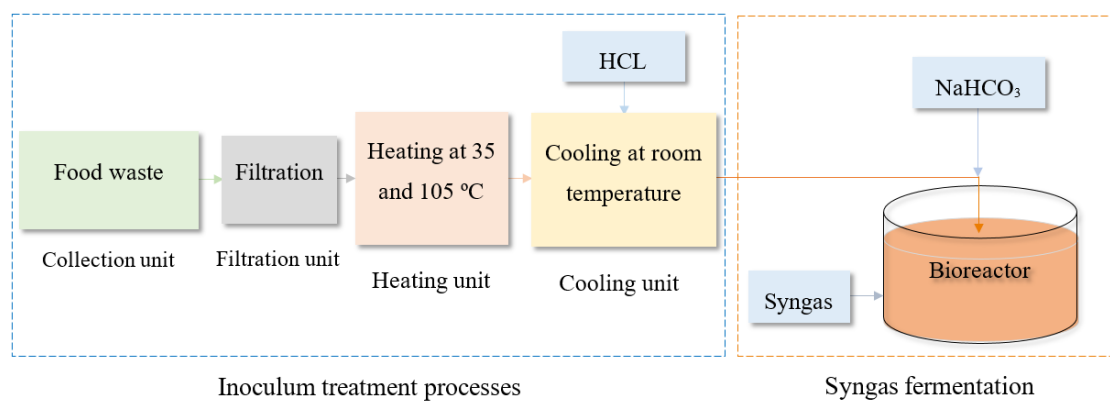
Figure 3.1: Flow diagram of overall syngas fermentation.

At first, 5 L of raw inoculum was filtered (600 µm) to eliminate large solid particles and kept the filtered inoculum in the closed bottle, to prevent over evaporation. The closed bottle was then incubated in an oven for 25 days at 35 ℃. The incubation process helps to activate the liquid media to produce left-over biogas, by enhancing digestion rate and bio-degradability. The closed bottle was equipped with a pipe on the top of the bottle to remove produced biogas. The inoculum was again heated up at 105 ℃ for 48 hours, to eliminate methanogenic bacteria. After a series of heat treatment processes, liquid media was left for cooling, and then adjusted pH (around 8) by adding hydrochloric acid (HCL). Finally, all the characteristics of inoculum such as pH, total chemical oxygen demand (COD_T), soluble chemical oxygen demand ($CODs$), volatile fatty acid (VFA), total solid (TS), total suspended solid (TSS), volatile solid (VS), volatile suspended solid (VSS), and alkalinity were tested before onset of experiment as shown in Table 3.1.

Table 3.1: Chemical parameters of inoculum before performing an experiment.

Characteristic of food waste (g/L)									Ethanol (pA*s)	pH
COD_T	$CODs$	TS	VS	TSS	VSS	Alkalinity	NH_4-N	Acetic acid		
13.8	6.9	12.3	7.5	5.3	3.9	3.5	1.96	1.893	13	7.98

3.2 Design, development, and test of bioreactor

3.2.1 Design and development of fermentation bioreactor

A laboratory-scale batch bioreactor was designed by keeping the following parameters in consideration: high-pressure resistance, gas and liquid leakage proof, flexible to handle, easy to assemble and disassemble, and safe to perform. The bioreactor, made from borosilicate glass of 4.14 L was used for the experiment. It consists of six small valves with equal size of 1.6 cm diameter and one main inlet valve of 4 cm diameter, as shown in Figure 3.2.
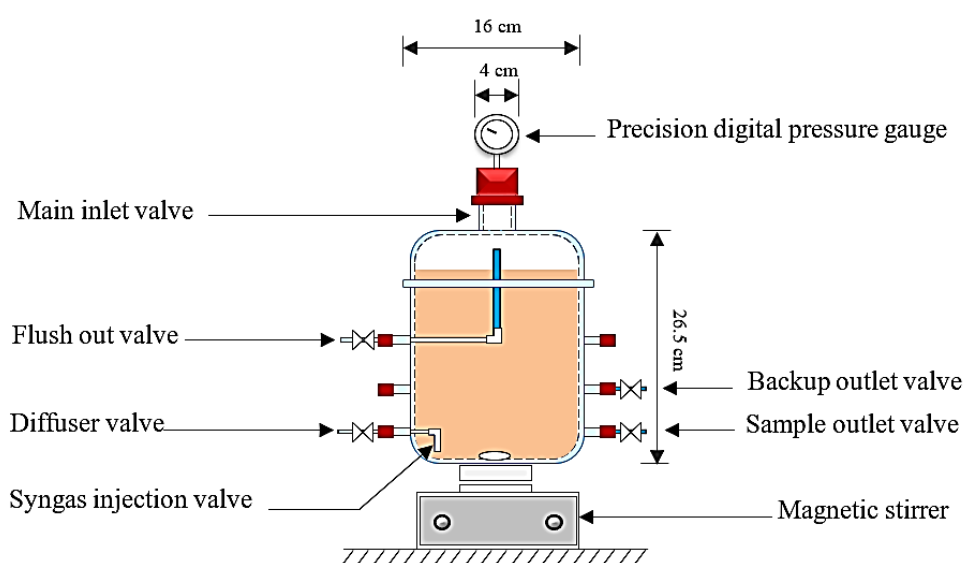
Figure 3.2: Schematic diagram of fermentation bioreactor.

The bioreactor working volume was designed of 3.25 L (i.e. 0.89 L headspace) and stirred continuously by a magnetic stirrer (MR 3001 K), range between 0 to 1200 rpm. The precision digital pressure gauge (model CPG1500), range from 0 to 10 bar, was installed on the top of the main inlet valve covered by a lid, to monitor total syngas pressure change. The lid consists of rubber cork, to hold pressure gauge tightly. To diffuse syngas in the liquid media homogeneously, a simple diffuser was designed at the bottom of the bioreactor, to enhance gas retention time. The flushing valve, 8 cm above from diffuser valve shown in Figure 3.2, was designed to flush the headspace air and bypass the headspace syngas in an emergency situation. The sampling valve was allocated at the right side of the bioreactor for taking a sample. All the possible openings/fissures of the bioreactor were sealed completely by Teflon/silicon, to prevent gas/liquid leakage in order to achieve anaerobic condition under high headspace pressure of 0.29 to 1.51 bar.

3.2.2 Lab-scale bioreactor design test

Before performing the experiment, it is an important to approve your designed and developed bioreactor, whether functioning well or not as your intended objective. Thus, after running the experiments, hydrogen seal test was performed inside the fume hood chamber, to investigate the bioreactor performance and sealing. The test lasted for three weeks. For the test, liquid media was used 3.25 L tap water, and hydrogen was used to pressurize the bioreactor at different headspace pressure of 0.33, 0.56, and 1.04 bars. During the tests, headspace pressure change was recorded each 10-minute interval and then analyzed the recorded data. The analyzed data showed that there was no gas and liquid leakage at high pressure the bioreactor was working well, the test report is attached in Appendix B. Therefore, the bioreactor was recommended for the master thesis experiment.

3.3 Experimental setup

The experiment was performed at University College of Southeast Norway (USN), Department of Energy and Environmental Technology, E-block, room number 113, from 9 Jan 2017 to 1 April 2017 (including hydrogen seal test). As mentioned in the previous section, the setup consists of 4.132 L bioreactor, integrated with a precision digital pressure gauge, shown in Figure 3.3a. The bioreactor was filled with 3.25 L of inoculum and added 3.4 g/L of sodium bicarbonate (as CO_2), as shown in Appendix C. The inoculum was agitated continuously.
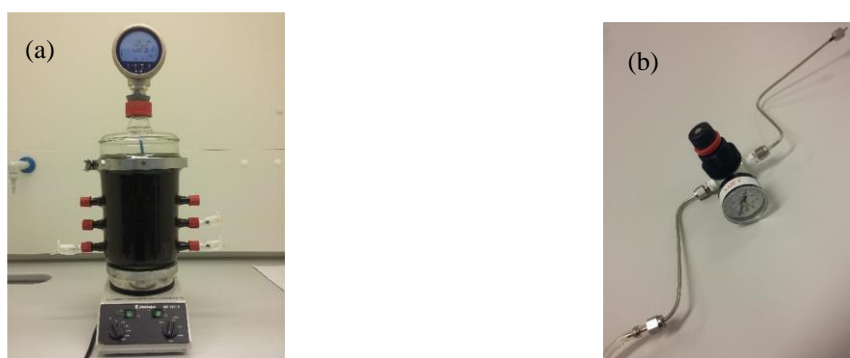
Figure 3.3: An overview of (a) Developed fermentation bioreactor. (b) Hague pipe with pressure regulator.

For the first time, headspace air was flushed with nitrogen, to achieve an anaerobic condition, and then supplied hydrogen 12 times to the headspace, at different headspace pressure range, between 0.29 to 1.51 bar. Hague pipe equipped with a pressure regulator to control flow rate was used to supply hydrogen into the bioreactor, shown in Figure 3.3b.

3.4 Batch fermentation of hydrogen and carbon dioxide

A laboratory scale batch experiment was conducted focusing primarily on hydrogen and carbon dioxide consumption. As described in above section, the bioreactor was filled with 3.25 L of

inoculum, in which 3.4 g/L of $NaHCO_3$ was added (when $NaHCO_3$ was added in the inoculum pH increased from 7.98 to 8.35). The headspace air was flushed once by nitrogen at the beginning, to create anaerobic condition and then supplemented hydrogen to the headspace several times at different headspace pressure range, between 0.29 to 1.51 bar. A digital pressure gauge was used to record the total pressure and temperature of the bioreactor.

The bioreactor was placed vertically inside the fume hood chamber and stirred continuously at the rate of 1200 rpm, to enhance the gas-liquid mass transfer. During the experiment, the headspace hydrogen diffused into the bulk liquid, inoculum, that caused a drop in headspace pressure. Therefore, hydrogen was injected several times until to achieve a steady state. During the experiments, each week, 10-20 mL of inoculum was taken for analysis and injected the same amount of freshly treated inoculum into the bioreactor in order to compensate the total working volume.

3.5 Volumetric mass transfer coefficients

The dynamic gassing out method was proposed to measure gas to liquid mass transfer capacity (k_La) [65], in which an increase of dissolved gas in the inoculum was recorded throughout the experiment. The same experiment described above was used for k_La measurement, too. To keep constant same mass transport, fermentation process was conducted at a stirrer speed of 1200 rpm and temperature of 22 ± 1.4 °C. Note that there was no any control device to keep the temperature constant, even though no significant changes were noticed during the fermentation. The headspace pressure was recorded each half hour using a digital pressure gauge during the experiment. Measured headspace pressure was subtracted with the initial headspace pressure to calculate dissolved hydrogen in the inoculum, and using the ideal gas law the dissolved hydrogen (bar) was converted into concentration (C_L) in mmol/L. To determine the volumetric mass transfer coefficient (k_La), Equation 3.1 was used (logarithm form after integration of Equation 2.1).

$$\ln(C^* - C_L) = -k_La * t \qquad \text{(Eq. 3.1)}$$

The calculation of the volumetric mass transfer coefficients will be discussed in Chapter 4, Section 4.3.

3.6 Solubility of gases in the liquid

The solubility of hydrogen was calculated based on headspace partial pressure of 0.29, 1.2, and 1.51 bar, caused by the dissolved hydrogen in the inoculum. The total headspace partial pressure was calculated by using the Dalton's law. The solubility of hydrogen in the inoculum was calculated using the Henry's law, as shown in Equation 3.2, [66].

$$C_H = k_{H,H_2} P_{Gas}$$
(Eq. 3.2)

where C_H is the solubility of hydrogen in a solvent (mol/L), k_{H,H_2} is Henry's coefficient (mol/atmL) and P_{Gas} is the partial pressure of gas (atm). The solubility of hydrogen in the inoculum will be discussed in Chapter 4, Section 4.4.

3.7 Analytical methods

3.7.1 Instrumental analysis

VFA (acetate, propionate, and butyrate) analysis

VFAs were analyzed by using gas chromatograph, Hewlett Packard 6890, equipped with a capillary column (FFAP, 30 m x 0.250 mm x 0.5 μm) and flame ionization detector with helium as a carrier gas, at a rate of 12 mL/minute. The injector and detector temperatures were set at 200ºC and 250ºC, respectively. The initial oven temperature 100ºC was maintained for a minute and raised 15 ºC per minute until 200 ºC, followed by an increase of 100ºC per minute until 230ºC.

pH analysis: pH was measured by calibrated Beckman 1051 pH meter at a room temperature.

3.7.2 Chemical parameters analysis

To determine chemical parameters US standards were used, as described in Table 3.2.

Table 3.2: List of US standards used for chemical parameters determination.

Description (Abbreviation)	Methods	Reference
Total Chemical Oxygen Demand (COD$_T$)	5220 D	[67, 68]
Soluble Chemical Oxygen Demand (COD$_S$)		
Ammonia (NH$_4^+$-N)	2500 A	[67]
Alkalinity	2320 B	[67, 69]
Total Solids (TS)	2540 B	[67]
Total Suspended Solids (TSS)	2540 D	[67]
Volatile Solids (VS)	2540 E	[67]
Volatile Suspended Solids (VSS)	2540 E	[67]

4 Results

4.1 Hydrogen consumption

A laboratory scale, batch fermentation was conducted to produce acetic acid and ethanol. The hydrogen was supplemented to the headspace and sodium bicarbonate (as CO_2 source) added in the inoculum. Figure 4.1a is an overview of hydrogen injection and consumption at headspace pressure ranged from 0.29 to 1.51 bar. Figure 4.1b shows the cumulative hydrogen consumption (mmol) during the experiment.
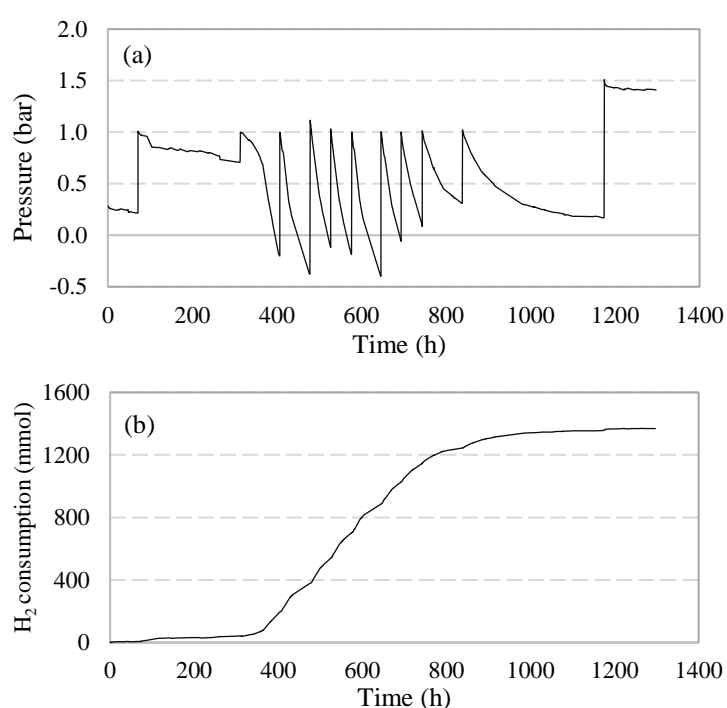
Figure 4.1: An overview of (a) Hydrogen injection and consumption. (b) Cumulative hydrogen consumption during the experiment.

The vertical and inclined line shown in Figure 4.1a indicates the hydrogen injection and consumption, respectively, at different headspace pressure of 0.29, 1.12, and 1.51 bar. During the experiment, 12 times, hydrogen was injected to the headspace. As can be seen in Figure 4.1a, approx. 1.12 bar of hydrogen was injected nine times during 300-1176 hours. Meanwhile, six times negative headspace pressure was noticed. The cumulative H_2 consumption trend was sigmoidal and found total H_2 consumption of 1369 mmol throughout the experiment, shown in Figure 4.1b. The dissolved hydrogen in the inoculum (H_2 consumption) experienced, a lag phase for the first 300 hours followed by sharp increase during 300-912 hours, and then depletion at later stages of the experiment. It was observed that the maximum H_2 consumption rate was 0.153 mmol/h·gVS during 478-527 hours at 1.12 bar headspace pressure, which was 51 times higher than that obtained during first 71 hours at 0.29 bar headspace pressure (0.003

19

mmol/h· gVS). The higher H_2 consumption rates were found in the middle stages of the experiment and then later stages of experiment H_2 consumption rates went down until to achieve a steady state as shown in Table 4.1.

Table 4.1: Average hydrogen consumption rates at different time intervals

Duration (h)	Hydrogen consumption rates		
	bar/h	mmol/h	mmol/h. gVS
Start-71	0.001	0.081	0.003
71-313	0.001	0.144	0.006
313-407	0.013	1.686	0.079
407-478	0.019	2.567	0.120
478-527	0.025	3.321	0.153
527-577	0.024	3.215	0.152
577-646	0.020	2.676	0.128
646-694	0.022	2.928	0.143
694-744	0.018	2.415	0.118
744-839	0.007	0.975	0.048
839-1174	0.003	0.336	0.017
1174-1297	0.001	0.107	0.005

4.2 Products formation

Two step reaction in the bioconversion process was followed to convert gases substrates into dissolved products, the microbial cells transport first gases substrates to the microbial surface and then the uptake of the soluble gases, to produce acetic acid and ethanol. Figure 4.2 shows the acetic acid and ethanol production, along with other organic acids.
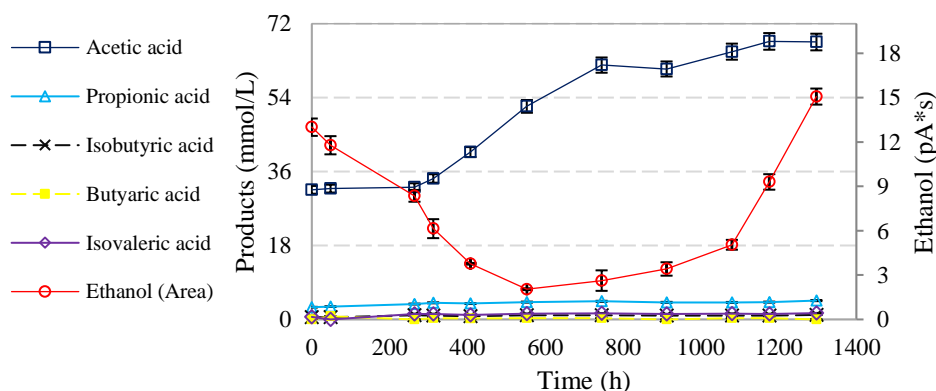
Figure 4.2: Concentration of acetic acid and ethanol. The error bar represents standard error, n = 3.

The initial acetic acid concentration was 32 mmol/L that increased rapidly between 264 to 745 hours, by 88 % from 33 to 62 mmol/L, albeit a long lag phase was noticed during first 300 hours. The maximum acetic acid concentration of 68 mmol/L was observed at 1176 hours and 1.12 bar headspace pressure and then declined slightly at the end of the experiment when H_2 consumption was no longer. The maximum rate of acetic acid formation was 0.0119 mmol/h·gVS at 1.12 bar headspace pressure during 408-553 hours, which was 15-folds higher than the least rate of 0.0008 mmol/h·gVS obtained at 0.29 bar headspace during first 48 hours, as shown in Table 4.2. During 1176-1297 hours, the acetic acid consumption rate of 0.0002 mmol/h·gVS was found at 1.51 bar headspace pressure. It is important to note that ethanol concentration decreased sharply at the beginning and reached the minimum level of 2.5 pA*s at 553 hours, which was approx. 6 times lower than the initial concentration (13 pA*s). Ethanol concentration was expressed in the area (pA*s). As can be seen in Figure 4.2, ethanol formation was lower, 2.5 to 3.4 pA*s, during 553 to 912 hours. However, at the later stages of experiment ethanol concentration increased exponentially and reached the maximum level of 15 pA*s at 1297 hours and 1.51 bar headspace pressure. The other organic acids, namely propionic, isobutyric, butyric, and isovaleric acid formation were also found almost constant but insignificant throughout the experiment, shown in Figure 4.2.

Table 4.2: Acetic acid formation rates at different time intervals.

Duration (h)	Acetic acid (mmol/h·gVS)	Acetic acid (mg/h.gVS)
Start-48	0.0008	0.0529
264-312	0.0068	0.4064
312-408	0.0112	0.6688
408-553	0.0119	0.7157
553-745	0.0083	0.4987
1080-1176	0.0042	0.2526
1176-1297	-0.0002	-0.0125
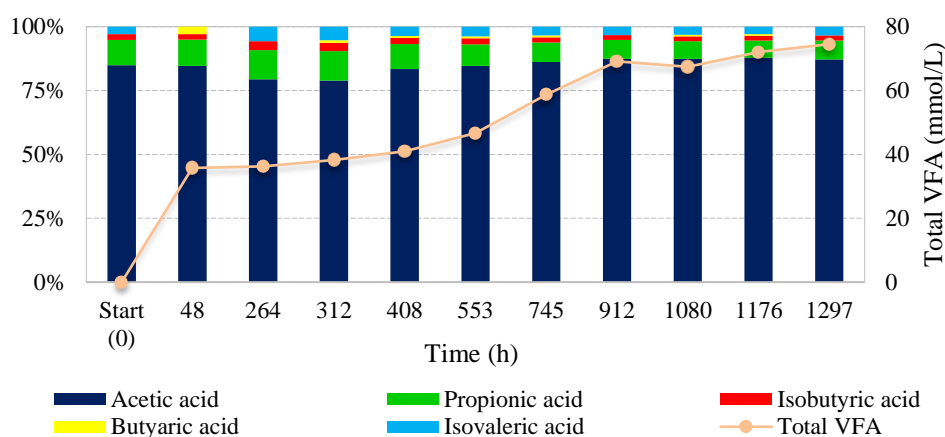
Figure 4.3: Concentration of VFA composition (%) during the fermentation.

Figure 4.3 shows the total VFA composition during the experiment. The decreasing trend of acetic acid concentration (%) in the total VFA was noticed for the first 312 hours; they were 85, 84, 79 and 78 %. However, the acetic acid was the dominant organic acid in total VFA throughout the experiment. Then, acetic acid concentration (%) increased gradually and reached up to the highest level, 88% at 1176 hours, when total VFA was 74 mmol/L at 1.12 bar headspace pressure. The maximum total VFA of 75 mmol/L was obtained at 1297 hours, which was 108% higher than the initial total VFA (36 mmol/L). It is also noticeable that the increasing trend of total VFA composition followed the similar pattern travelled by acetic acid formation (Fig. 4.2).

Figure 4.4a and Figure 4.4b show the COD_S and COD_T concentrations and NH_4-N and pH, respectively, during the experiment.
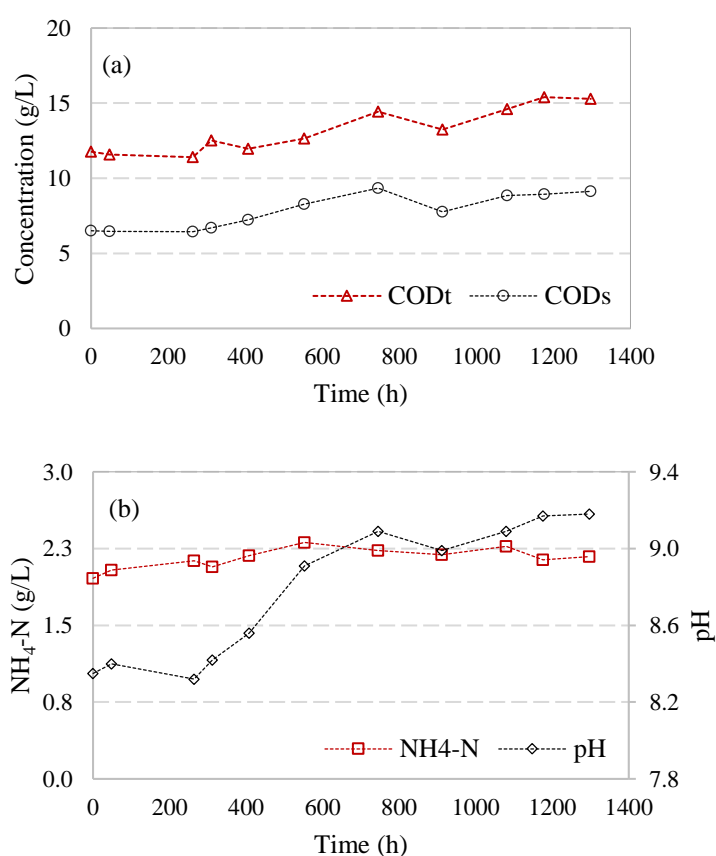
Figure 4.4: Profile of (a) COD_T and COD_S concentrations. (b) NH_4-N and pH.

The COD_T and COD_S concentrations shown in Figure 4.4a followed similar trend travelled by acetic acid. The maximum COD_T and COD_S concentrations were 15.4 and 9.4 g/L at 1176 and 745 hours, and increased by 30 and 40%, respectively. The total consumed hydrogen COD ($COD_{Hydrogen}$) was 11.02 gCOD, which was approx. equal to total produced inoculum COD ($COD_{Inoculum}$ = 11.44 gCOD) and 32% more than the total produced acetic acid COD ($COD_{Acetic\ acid}$ = 7.49 gCOD) during the fermentation, as shown in Appendix D. The NH_4-N concentration was noticed almost constant between 1.9 to 2.3 g/L. The maximum NH_4-N concentration of

2.3 g/L was obtained at 553 hours. As can be observed in Figure 4.4b, pH increased from 8.35 to 9.18 during the experiment, although a couple of time (264 and 912 hours) pH drop was noticed. It was noticeable that the pH increased substantially during 264-745 hours. In addition, increased alkalinity concentration was found during the experiment, initial and final alkalinity concentrations were 3.15 and 4.7 g/L, respectively.

Figure 4.5a and Figure 4.5b show the profile of TSS, VSS, TS, and VS concentrations throughout fermentation.
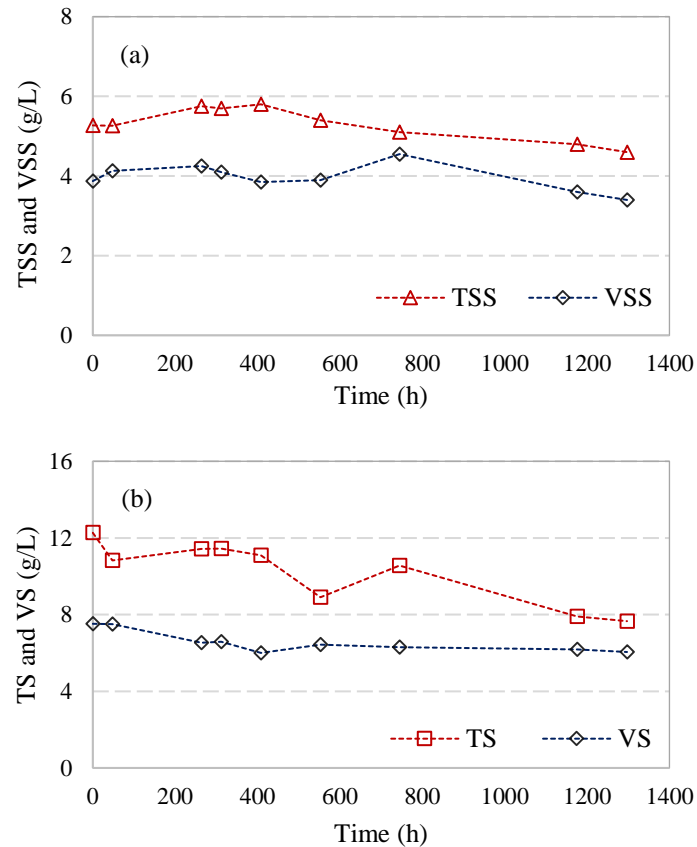
Figure 4.5: Profile of (a) TSS and VSS. (b) TS and VS.

As shown in Figure 4.5a, TSS and VSS reduction was noticed during the experiment. The reduced TSS and VSS were 15 (0.8 g/L) and 13% (0.5 g/L), respectively. However, a small increment of TSS and VSS were observed from 264 to 745 hours. Similarly, TS and VS reduction was also noticed and found total reduction of 38 (4.6 g/L) and 20% (1.5 g/L), respectively. Couple times, at 48 and 553 hours, quick decline in TS concentration was noticed, as shown in Figure 4.5b. As can be seen in both Figure 4.5a and Figure 4.5b, total TSS and TS reduction were higher than total VSS and VS reduction, respectively, throughout experiment.

4.3 Volumetric mass transfer coefficients

Figure 4.6a, Figure 4.6b, and Figure 4.6c show the volumetric mass transfer coefficient of hydrogen in the inoculum at different headspace pressure of 0.29, 1.12, and 1.51 bar, respectively, during the experiment.
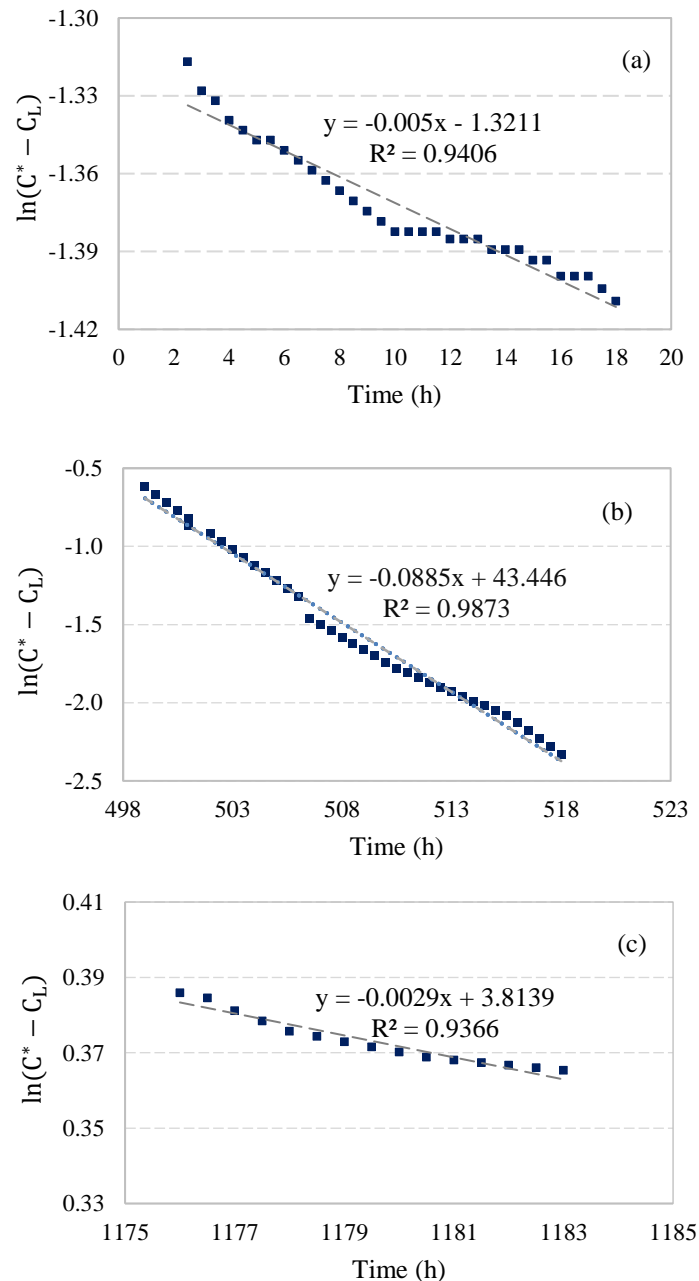
Figure 4.6: The volumetric mass transfer coefficients of hydrogen in the inoculum. (a) at 0.29 bar. (b) at the 1.12 bar. (c) at 1.51 bar.

In all of Figure 4.6, $\ln(C^* - C_L)$ vs. time gives a straight line with a slope that equals to the volumetric mass transfer coefficients of hydrogen in the inoculum $(k_L a)$. In our studies, the $k_L a$ was measured at where dissolved hydrogen concentration rate was maximum at three different headspace pressure of 0.29, 1.12, and 1.51 bar. The dissolved hydrogen concentration rates were found maximum during 2-20, 498-518, and 1176-1183 hours. The $k_L a$ was observed increasing with an increase of headspace pressure from 0.29 to 1.12 bar. The volumetric mass transfer coefficients were 0.005 h^{-1} ($R^2 = 0.941$) at 0.29 bar headspace pressure and 0.16 mmol/L dissolved hydrogen concentration during first 20 hours, shown in Figure 4.6a. The maximum $k_L a$ 0.082 h^{-1} ($R^2 = 0.987$) was obtained at 1.12 bar headspace pressure and 89 mmol/L dissolved hydrogen concentration during 498-518 hours, shown in Figure 4.6b. However, the least was found 0.003 h^{-1} ($R^2 = 0.937$) at 1.51 bar headspace pressure and 419 mmol/L dissolved hydrogen concentration during 1176-1183 hours, shown in Figure 4.6c.

4.4 Solubility of gases in the liquid

Figure 4.7 shows the temperature changes, between 20.6 to 23.4 °C, during the experiment.
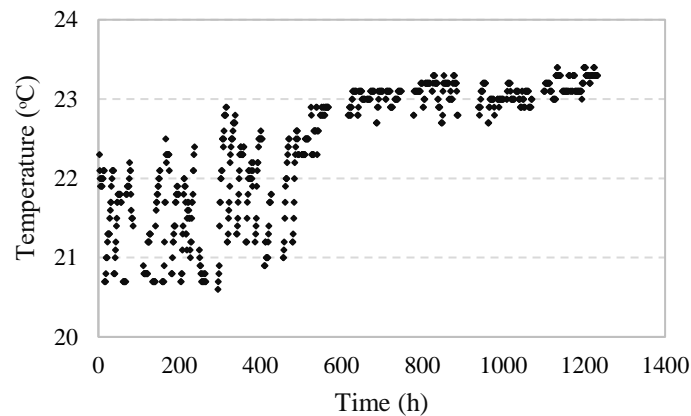
Figure 4.7: Change in bioreactor temperature over time.

The bioreactor temperature was observed changing with an increase in headspace pressure. The maximum temperature fluctuation (20.6 to 22.6°C) was noticed for first 502 hours at headspace pressure between 0.29-1.12 bar. The temperature reached up to 23.4°C when headspace pressure was 1.51 bar. The average temperatures during 0-300, 300-1176, and 1176-1297 hours were 21.6, 22.3, and 23.1°C at headspace pressure of 0.29, 1.12, and 1.51 bar, respectively, shown in Figure 4.7.

The solubility of hydrogen in the inoculum (C_H) was calculated using Equation 3.2, under anaerobic condition. Henry's coefficient for hydrogen, 7.8 10^{-4} mol/atmL at 295.65 K, was used [66]. The C_H at three different headspace pressure was measured during 0-71, 478-527, and 1176-1297 hours (Table 4.3). Durations were chosen based on higher hydrogen consumption rate at three different headspace pressure ranged from 0.29, 1.12, and 1.51 bar. The C_H was found increasing with an increase of headspace pressure.

Table 4.3: The calculated solubility of hydrogen in the inoculum at different headspace pressure.

Headspace pressure (bar)	Time interval (h)	Temperature (ºC)	Hydrogen consumption rate (mmol/h· gVS)	Solubility of hydrogen in liquid (mol/L)
0.29	0-71	21.6	0.003	4.9×10^{-5}
1.12	478-527	22.3	0.153	1.2×10^{-3}
1.51	1176-1297	23.1	0.005	7.7×10^{-5}

Figure 4.8 shows the solubility of hydrogen in the inoculum at different headspace pressure and dissolved hydrogen.
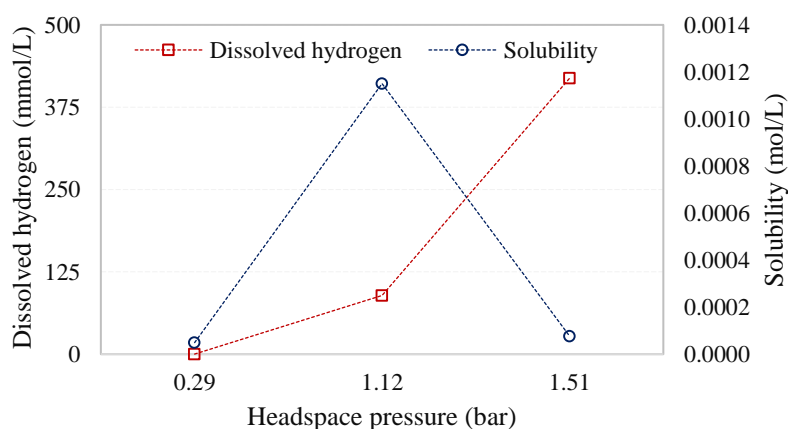
Figure 4.8: The solubility of hydrogen in the inoculum at different headspace pressure.

The maximum C_H 1.2×10^{-3} mol/L was obtained at 1.12 bar headspace pressure (89 mmol/L dissolved hydrogen), which was 25 and 16 times higher than that obtained at 0.29 bar (0.16 mmol/L dissolved hydrogen concentration) and 1.51 bar headspace pressure (419 mmol/L dissolved hydrogen concentration), respectively. The results showed that an increase of dissolved hydrogen concentration in the inoculum at a level of saturation point reduced the C_H value. In contrast to dissolved hydrogen concentration, increasing headspace pressure resulted in increased C_H value, shown in Figure 4.8. The overall solubility of hydrogen in the inoculum was 8.03×10^{-3} mol/L during the experiment, as shown in Appendix E.

4.5 Biomass growth and stoichiometry reaction

4.5.1 Biomass yield and stoichiometry reaction of acetic acid formation

The microbial synthesis of acetic acid is growth related [70]. Microorganism growth is thus clung to the production of acetic acid. The stoichiometry reaction 4.1 was derived based on reaction 2.5. The biomass yield was calculated in the presence of hydrogen gas as an electron

donor, associated stoichiometrically with acetic acid formation, calculation is included in Appendix F. The $C_5H_7O_2N$ was used as a biomass for cell yield on gases substrates [64].

$$277.78H_2 + HCO_3^- + NH_4^+ + 137.88CO_2 \rightarrow C_5H_7O_2N + 66.94CH_3COOH + 142.89H_2O$$

(R. 4.1)
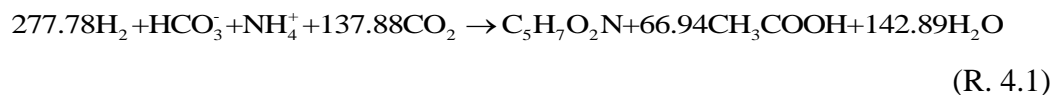
All the parameters defined in Table 4.4 were assumed to calculate biomass yields along with acetic acid production, based on the chemical oxygen demand.

Table 4.4: An overview of parameter values.

Parameter	Value (unit)
Energy transfer efficiency (ε)	0.1 to 1, Assumption
Free energy, reduction N_2 to NH_4^+ (ΔG_{PC})	18.8 kJ/e⁻eq [71]
Free energy, carbon to pyruvate (ΔG_P)	74.96 kJ/e⁻eq (H_2, electron donor)
Biomass $C_5H_7O_2N$ (1 g cells)	1.42 gCOD/g compound

The biomass yields were calculated, at a various range of energy transfer efficiency (0.1 to 1), correlated stoichiometrically with ethanol formation. The calculation is attached in Appendix F.

Figure 4.9 shows the biomass yield vs. energy transfer efficiency ranged from 0.1 to 1, along with acetic acid formation.
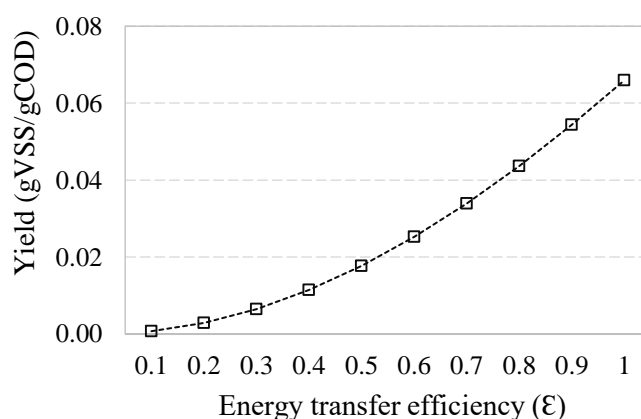
Figure 4.9: Biomass yield associated with the acetic acid formation.

The increase in energy transfer efficiency increased the biomass yield, shown in Figure 4.9. The biomass yield of 0.066 gVSS/gCOD (maximum) was found at 1 energy transfer efficiency and the least was 0.001 gVSS/gCOD at 0.1 energy transfer efficiency.

4.5.2 Biomass yield and stoichiometry reaction of ethanol formation

The stoichiometry reaction 4.2 was derived from reaction 2.8. A similar method as described above was used here also to formulate stoichiometry reaction for biomass growth associated with ethanol formation (Appendix F). Microorganisms can grow on H_2 and CO_2, with the absence of CO. Therefore, we are more interested in ethanol production from CO_2, using hydrogen as an electron donor.

$$312.5H_2 + HCO_3^- + NH_4^+ + 104.63CO_2 \rightarrow C_5H_7O_2N + 50.38CH_3COOH + 160.25H_2O$$

(R. 4.2)
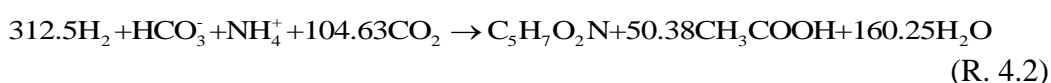
The biomass growths were calculated, on assumption of free energy transfer efficiency ranged from 0.1 to 1, along with ethanol formation, using above listed parameters value, (Table 4.4). The calculation is attached in Appendix F.

Figure 4.10 shows the increasing trend of biomass yield with an increase in energy transfer efficiency, ranged from 0.1 to 1.
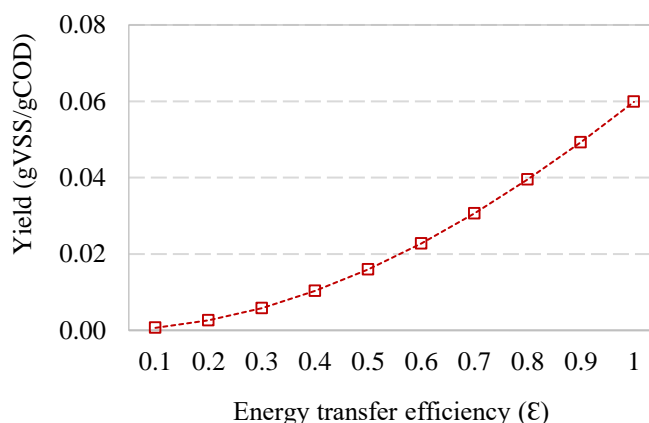
Figure 4.10: Biomass yield associated with ethanol formation.

The biomass yield presented in Figure 4.10 shows that increase of energy transfer efficiency (0.1 to 1) increased the biomass yield, during ethanol formation. The highest and the lowest biomass yield were found 0.059 and 0.001 gVSS/gCOD at 1 and 0.1 energy transfer efficiency, respectively.

5 Discussion

5.1 Hydrogen consumption

As noticed in Figure 4.1a, increasing headspace pressure resulted in an increased H_2 consumption during the experiment. This trend leads to dissolved hydrogen in the inoculum is governed by headspace pressure [33]. The lag phase was experienced for first 300 hours because of microorganisms needed time to acclimate to a new environment. Thus H_2 consumption was found low [64]. Also, other expected reason could be a low mass transfer rate from gases to liquid phase due to low initial headspace pressure of 0.29 bar [14, 33]. During 300-1176 hours, H_2 consumption was found maximum at headspace pressure of approx. 1.12 bar. The main reason could be the microorganism cells increasing at their optimum rate and an increased mass transfer rate from gases to liquid phase due to an increased headspace pressure [14, 33, 64]. This result postulates that an increase in H_2 consumption is a result of an increase in headspace pressure [33]. As shown in Figure 4.1a, H_2 consumption was decreased gradually and achieved a steady state after 1176 hours. The stationary phase and increased pH (pH>9) could be the reason of decreased H_2 consumption. In the stationary phase, the microorganism growth is offset by cells death (no extra cells growth) [64, 72], and excessive increase of pH hinders the microorganisms' capacity for H_2 consumption [33].

5.2 Products formation

A laboratory scale, batch fermentation was performed at headspace pressure ranged from 0.29 to 1.51 bar, where hydrogen and carbon dioxide served as an electron and energy source for acetic acid and ethanol formation under acetyl-CoA pathway. As observed in Figure 4.2, acetic acid and ethanol formation were found during the experiment. Increasing H_2 consumption resulted in increased acetic acid formation, that postulates an increase of acetic acid formation depends on H_2 consumption at headspace pressure [33, 60]. Acetic acid formation started after 300 hours. An initial lag phase might be the reason of delayed acetic acid formation, during that interval H_2 consumption was significantly low [64]. High acetic acid formation was found during 300-745 hours and reached the maximum level at 1176 hours, then declined slightly at later periods of fermentation, shown in Figure 4.2. An increased acetic acid formation was due to the increased H_2 consumption rate [33]. After 1176 hours of fermentation, acetic acid consumption was observed. It could be a consequence of acetic acid conversion into ethanol according to the acetogenic pathway, to avoid of high undissociated acetic acid accumulation or nutrient limitation [33, 59, 73-75].

Regarding ethanol formation, the metabolic shift from acetic acid to ethanol (acidogenic to solventogenic phase) was obtained at a pH of 9.09, headspace pressure of 1.12 bar. As shown in Figure 4.2, exponential ethanol formation was noticed after 745 hours. The sharp increase of ethanol concentration might be a result of increased headspace pressure from 1.12 to 1.51 bar [9, 33, 76]. A similar experiment examined by Younesi et al. [33], they found 4-folds higher ethanol concentration at total syngas pressure of 1.6 and 1.8 atm than at 0.8 and 1 atm. In addition, several studies showed that an increase of solventogenesis is sporulation-associated [77, 78]. Thus, sudden ethanol formation in our case might be a consequence of onset of

solventogenesis. During the first 553 hours, ethanol concentration was consumed gradually by microorganisms and remained almost constant (lowest) between 553 to 912 hours. The observed ethanol reduction could be the result of increased pH [32, 33]. Despite intensive research, it is hard to explain clearly why ethanol consumption occurred at the beginning. But, sporulation could be a reason for constant ethanol concentration in the middle of fermentation. Microorganisms are no longer active for reaction for ethanol formation when sporulation occurred [32].

As can be seen in Figure 4.4a, both COD_T and COD_S concentrations of inoculum increased, during the experiment, due to consumption of hydrogen and carbon dioxide for acetic acid and ethanol formation. During the experiment, total consumed hydrogen COD ($COD_{Hydrogen}$) was nearly equivalent to the increase in bulk liquid COD ($COD_{Inoculum}$). At least 68 % of $COD_{Hydrogen}$ transformed to acetic acid concentration ($COD_{Acetic\ acid}$), that implies 32% of the total consumed hydrogen ($COD_{Hydrogen}$) converted to other final products, such as ethanol, propionic, isobutyric, butyric, and isovaleric acid).

Since the experiment was performed at high pH, acetic acid and ethanol formations were observed, during the experiment. Previous studies suggested that decrease in pH attributes to the formation of organic acids and phase change from acidogenesis to solventogenesis for ethanol production [9, 32, 38]. However, in our case, pH increased from 8.35 to 9.18 during the experiment as shown in Figure 4.4b. During the fermentation, an increase of pH could happen if added buffer solution lost their capacity to resist inoculum pH change that leads to regaining initial pH level [79], which was shown after 745 hours (initially, HCL was added to control pH as required level). Furthermore, sodium bicarbonate (as CO_2) addition could be another reason of increased pH and alkalinity, sodium and bicarbonate are the base and acid components, respectively. When bicarbonate was used as a CO_2 source for acetic acid and ethanol formation, only base component remained. Thus, pH increased and inoculum became more alkaline [80]. However, in order to confirm these assumptions, more intensive research would require to be performed.

As noted in Figure 4.5a and Figure 4.5b, TSS, VSS, and TS, VS reduction were observed throughout fermentation. The observed solids (TSS, VSS, and TS, VS) reduction can be the result of acetic acid, ethanol, and other organic acids formation [79]. During the experiment, TSS and TS reductions were higher than VSS and VS reductions, respectively. This could happen due to TSS and TS reductions include not only organic matter degradation (VSS and VS reduction) but also includes inorganic suspended particles degradation [79, 81].

5.3 Volumetric mass transfer coefficients

The volumetric mass transfer coefficient $(k_L a)$ increases with an increase in both gas and liquid flow rate, caused by an increased mass transfer efficiency (k_L) and specific interfacial area (a) [82, 83]. Previous studies showed that the $k_L a$ could be enhanced either by increasing agitation speed or by gas flow rate [14]. An increasing headspace pressure resulted in increased gas flow rate. As noticed in Figure 4.6, increasing headspace pressure increased the $k_L a$ value. This indicates that transform of gases to liquid phase depends on the headspace pressure [32]. This could be the reason of maximum $k_L a$ value at 1.12 bar headspace pressure, in our case. The $k_L a$ value was found the lowest, even though headspace pressure was highest (1.51 bar

headspace pressure). It could happen if the dissolved gases concentration in the liquid already reached saturation level, no more gas is possible to dissolve in the liquid [32]. In our studies, hydrogen consumption rate reached a steady state after 1176 hours at 1.15 bar headspace pressure due to enough dissolved hydrogen present in the inoculum (419 mol/L). Thus, this could be a result of $k_L a$ value at the later stage of the experiment.

5.4 Solubility of gases in the liquid

From experimental results presented in above Chapter shows that the solubility of hydrogen in the inoculum (C_H) increases with headspace partial pressure. These trends indicate that the solubility of hydrogen is governed by the headspace partial pressure [66, 84, 85]; increasing partial pressure forces the hydrogen molecules into the inoculum, causes more H_2 consumption. These could be the cause of maximum C_H value at 1.12 bar headspace pressure and 22.3ºC, during the experiment. On the contrary, the lowest was found at 1.51 bar headspace pressure and 23.1ºC after 1174 hours of the experiment. Many studies found that the solubility of gas in a liquid depends on the nature of solution and temperature, an increase of dissolved gas in the liquid changes physical state of solution that results in a reduction of the solubility of gas in liquid [66, 86]. As shown in Figure 4.1b, the H_2 consumption rate was observed minimum after 1176 hours due to enough hydrogen already dissolved in the inoculum (419 mol/L). This could be a consequence of low solubility of hydrogen in the inoculum.

5.5 Biomass growth and stoichiometry reaction

5.5.1 Biomass yields and stoichiometry of acetic acid formation

Acetogenic bacteria is broken down by acidogenesis for acetic acid production, in acetyl-CoA pathway [70]. An increase of substrates consumption increases the acetic acid formation and biomass yields [33]. As given by stoichiometry reaction 4.1, biomass yield was correlated stoichiometrically with the acetic acid formation and had no hydrogenase inhibition due to the fact that in this fermentation no carbon monoxide was added [32]. The increase in energy transfer efficiency without hydrogenase inhibition would increase substrate utilization for rapid cell synthesis. As a result, biomass yield increased sharply.

5.5.2 Biomass yields and stoichiometry of ethanol formation

Ethanol formation occurs in solventogenesis phase, along with biomass cell growth, in acetyl-CoA pathway [70]. In the fermentation process, pH drop not only switches acidogenesis to solventogenesis phase for ethanol production but also reduces the biomass cell growth [9, 38]. Therefore, it could be the reason for less biomass yield compared to biomass yield associated with the acetic acid formation. As given by stoichiometry reaction 4.2, biomass cell growth is associated with ethanol formation. As discussed above, an increase of energy transfer efficiency increases substrates consumption for cells synthesis, thus biomass yield increased.

6 Conclusion and recommendation

6.1 Conclusion

The primary purpose of this master thesis was to gain a better understanding of acetic acid and ethanol production via an experimental approach, "syngas fermentation". The experiment was successfully performed and drawn the following key conclusions:

- **Increasing headspace pressure enhanced the hydrogen consumption.** Maximum H_2 consumption rate was observed 0.153 mmol/h·gVS at 1.12 bar headspace pressure during 478-527 hours, which was 51% more than that obtained at 0.29 bar headspace pressure during first 71 hours.

- **Enhanced hydrogen consumption increased the acetic acid formation.** Maximum acetic acid formation rate was 0.0119 mmol/h·gVS at 1.12 bar headspace pressure, which was 15-folds more than that of obtaining at 0.29 bar headspace pressure (0.0008 mmol/h· gVS). At least 68% of consumed hydrogen ($COD_{Hydrogen}$ = 11.02 gCOD) transformed to acetic acid ($COD_{Acetic\ acid}$ = 7.44 gCOD) and found a maximum acetic acid concentration of 68 mmol/L at 1176 hours and headspace pressure ranged from 0.29-1.51 bar during the fermentation.

- **Headspace pressure significantly influenced the ethanol formation.** A significant ethanol consumption was appeared during first 553 hours at headspace pressure between 029-1.12 bar. However, ethanol formation was found at the later stages of fermentation and obtained a maximum concentration of 15 pA*s at 1.51 bar headspace pressure and 1297 hours, which was 7 times higher than obtained the least ethanol concentration at 1.12 bar headspace pressure and 553 hours.

- **The increase of headspace pressure had a significant influence on the mass (H_2) transfer from gases to liquid phase ($k_L a$) and solubility of gases in liquid (C_H).** An increase of headspace pressure resulted in increased $k_L a$ and C_H value. Maximum $k_L a$ and C_H were observed 0.082 h^{-1} (R^2 = 0.987) and 1.12 10^{-3} mol/L at headspace pressure increased from 0.29 to 1.12 bar, during 478-527 hours. However, increasing dissolved hydrogen concentration in the inoculum showed the inverse results.

- **Biomass yield can be optimized, with an increase of energy transfer efficiency (ε).** The calculated maximum biomass yields were 0.066 gVSS/gCOD and 0.059 gVSS/gCOD, for acetic acid and ethanol formation, respectively, when the assumption of ε was 100%.

- Solids reduction (TSS = 15%, VSS = 13%, TS = 38%, and VS = 20%) and pH increment ranged from 8.35-9.18 were observed during the experiment.

6.2 Recommendation

The dissertation emphasizes acetic acid and ethanol production through microbial hydrogen and carbon dioxide fermentation. The purposed objectives were fulfilled successfully, based on experimental approach. However, there were few issues noticed which are recommended as follows for future research:

- **The inclusion of carbon monoxide fermentation.** The current experiment was performed using hydrogen gas and sodium bicarbonate (as CO_2). The use of CO as substrate was originally planned for this project, but it was delayed because of the complexity of such experiments, related to safety. CO is suggested to be included as a substrate for further research.

- **Further research on high pH (pH>8) microbial fermentation.** Most of the research are focused on H_2, CO_2, and CO fermentation at low pH. Few or almost no research is done on high pH microbial fermentation. Therefore, it would be beneficial to perform high pH content fermentation in the future to acquire the better understanding of such fermentation.

- **Longer experimental time would be required for complete ethanol formation.** The ethanol production was seen at the later stages of fermentation. The schedule of time was not enough for ethanol formation, the trend showed it needs more time for complete ethanol formation. Therefore, allocation of longer experimental time is suggested to be applied for same nature of the future experiment.

References

[1]   A. i. d. l'énergie, *Energy technology perspectives 2012: pathways to a clean energy system*: OECD/IEA, 2012.

[2]   European-Union, "Directive of the European Parliament and of the Council of 23 April 2009 on the Directives, promotion of the use of energy from renewable sources and amending and subsequently repealing 2001/77/EC and 2003/30/EC," 2009.

[3]   J. Daniell, M. Köpke, and S. D. Simpson, "Commercial biomass syngas fermentation," *Energies,* vol. 5, pp. 5372-5417, 2012.

[4]   F. Cherubini, "The biorefinery concept: using biomass instead of oil for producing energy and chemicals," *Energy Conversion and Management,* vol. 51, pp. 1412-1421, 2010.

[5]   D. K. Kundiyana, R. L. Huhnke, and M. R. Wilkins, "Syngas fermentation in a 100-L pilot scale fermentor: design and process considerations," *Journal of bioscience and bioengineering,* vol. 109, pp. 492-498, 2010.

[6]   E. van Steen and M. Claeys, "Fischer-Tropsch Catalysts for the Biomass-to-Liquid (BTL)-Process," *Chemical engineering & technology,* vol. 31, pp. 655-666, 2008.

[7]   M. D. Bredwell, P. Srivastava, and R. M. Worden, "Reactor design issues for synthesis-gas fermentations," *Biotechnology progress,* vol. 15, pp. 834-844, 1999.

[8]   M. Saritha and A. Arora, "Biological pretreatment of lignocellulosic substrates for enhanced delignification and enzymatic digestibility," *Indian journal of microbiology,* vol. 52, pp. 122-130, 2012.

[9]   K. T. Klasson, M. D. Ackerson, E. C. Clausen, and J. L. Gaddy, "Bioconversion of synthesis gas into liquid or gaseous fuels," *Enzyme and Microbial Technology,* vol. 14, pp. 602-608, 1992.

[10]   L. R. Formenti, A. Nørregaard, A. Bolic, D. Q. Hernandez, T. Hagemann, A. L. Heins*, et al.*, "Challenges in industrial fermentation technology research," *Biotechnology journal,* vol. 9, pp. 727-738, 2014.

[11]   P. C. Munasinghe and S. K. Khanal, "Biomass-derived syngas fermentation into biofuels: Opportunities and challenges," *Bioresource Technology,* vol. 101, pp. 5013-5022, 7// 2010.

[12]   H. N. Abubackar, M. C. Veiga, and C. Kennes, "Biological conversion of carbon monoxide: rich syngas or waste gases to bioethanol," *Biofuels, Bioproducts and Biorefining,* vol. 5, pp. 93-114, 2011.

[13]   R. K. Thapa, C. Pfeifer, and B. M. Halvorsen, "Flow Regime Identification in a Fluidized Bed Combustion Reactor," *International Journal of Modeling and Optimization,* vol. 6, p. 188, 2016.

[14]   Y. Shen, "Attached-growth bioreactors for syngas fermentation to biofuel," 2013.

[15]   O. Meyer and H. G. Schlegel, "Biology of aerobic carbon monoxide-oxidizing bacteria," *Annual Reviews in Microbiology,* vol. 37, pp. 277-310, 1983.

[16] M. Gnida, R. Ferner, L. Gremer, O. Meyer, and W. Meyer-Klaucke, "A novel binuclear [CuSMo] cluster at the active site of carbon monoxide dehydrogenase: characterization by X-ray absorption spectroscopy," *Biochemistry,* vol. 42, pp. 222-230, 2003.

[17] R. Si and M. Flytzani-Stephanopoulos, "Shape and Crystal-Plane Effects of Nanoscale Ceria on the Activity of Au-CeO2 Catalysts for the Water–Gas Shift Reaction," *Angewandte Chemie,* vol. 120, pp. 2926-2929, 2008.

[18] E. Pezacka and H. G. Wood, "Role of carbon monoxide dehydrogenase in the autotrophic pathway used by acetogenic bacteria," *Proceedings of the National Academy of Sciences,* vol. 81, pp. 6261-6265, 1984.

[19] L. Ljungdhal, "The autotrophic pathway of acetate synthesis in acetogenic bacteria," *Annual Reviews in Microbiology,* vol. 40, pp. 415-450, 1986.

[20] S. W. Ragsdale and E. Pierce, "Acetogenesis and the Wood–Ljungdahl pathway of CO 2 fixation," *Biochimica et Biophysica Acta (BBA)-Proteins and Proteomics,* vol. 1784, pp. 1873-1898, 2008.

[21] J. L. Gaddy, D. K. Arora, C.-W. Ko, J. R. Phillips, R. Basu, C. V. Wikstrom*, et al.*, "Methods for increasing the production of ethanol from microbial fermentation," ed: Google Patents, 2007.

[22] K. Schuchmann and V. Müller, "Autotrophy at the thermodynamic limit of life: a model for energy conservation in acetogenic bacteria," *Nature Reviews Microbiology,* vol. 12, pp. 809-821, 2014.

[23] M. Köpke, C. Mihalcea, J. C. Bromley, and S. D. Simpson, "Fermentative production of ethanol from carbon monoxide," *Current opinion in biotechnology,* vol. 22, pp. 320-325, 2011.

[24] F. R. Bengelsdorf, M. Straub, and P. Dürre, "Bacterial synthesis gas (syngas) fermentation," *Environmental technology,* vol. 34, pp. 1639-1651, 2013.

[25] A. Das and L. G. Ljungdahl, "Clostridium pasteurianum F1Fo ATP synthase: operon, composition, and some properties," *Journal of bacteriology,* vol. 185, pp. 5527-5535, 2003.

[26] W. Buckel and R. K. Thauer, "Energy conservation via electron bifurcating ferredoxin reduction and proton/Na+ translocating ferredoxin oxidation," *Biochimica et Biophysica Acta (BBA)-Bioenergetics,* vol. 1827, pp. 94-113, 2013.

[27] H. Latif, A. A. Zeidan, A. T. Nielsen, and K. Zengler, "Trash to treasure: production of biofuels and commodity chemicals via syngas fermenting microorganisms," *Current Opinion in Biotechnology,* vol. 27, pp. 79-87, 6// 2014.

[28] E. Biegel, S. Schmidt, J. M. González, and V. Müller, "Biochemistry, evolution and physiological function of the Rnf complex, a novel ion-motive electron transport complex in prokaryotes," *Cellular and molecular life sciences,* vol. 68, pp. 613-634, 2011.

[29] F. Imkamp and V. Müller, "Chemiosmotic energy conservation with Na+ as the coupling ion during hydrogen-dependent caffeate reduction by Acetobacterium woodii," *Journal of bacteriology,* vol. 184, pp. 1947-1951, 2002.

[30] M. Köpke, C. Held, S. Hujer, H. Liesegang, A. Wiezer, A. Wollherr*, et al.*, "Clostridium ljungdahlii represents a microbial production platform based on syngas," *Proceedings of the National Academy of Sciences,* vol. 107, pp. 13087-13092, 2010.

[31] K. M. Hurst and R. S. Lewis, "Carbon monoxide partial pressure effects on the metabolic process of syngas fermentation," *Biochemical Engineering Journal,* vol. 48, pp. 159-165, 1/15/ 2010.

[32] J. Vandecasteele, "Experimental and modelling study of pure-culture syngas fermentation for biofuels production," 2016.

[33] H. Younesi, G. Najafpour, and A. R. Mohamed, "Ethanol and acetate production from synthesis gas via fermentation processes using anaerobic bacterium, Clostridium ljungdahlii," *Biochemical Engineering Journal,* vol. 27, pp. 110-119, 2005.

[34] B. H. Kim, P. Bellows, R. Datta, and J. Zeikus, "Control of carbon and electron flow in Clostridium acetobutylicum fermentations: utilization of carbon monoxide to inhibit hydrogen production and to enhance butanol yields," *Applied and environmental microbiology,* vol. 48, pp. 764-770, 1984.

[35] B. E. Skidmore, "Syngas fermentation: Quantification of assay techniques, reaction kinetics, and pressure dependencies of the clostridial P11 hydrogenase," 2010.

[36] F. M. R. Pereira, M. Alves, and D. Sousa, "Effect of pH and pressure on syngas fermentation by anaerobic mixed cultures," in *13th World Congress on Anaerobic Digestion*, 2013, pp. 1-4.

[37] H. N. Abubackar, M. C. Veiga, and C. Kennes, "Biological conversion of carbon monoxide to ethanol: effect of pH, gas pressure, reducing agent and yeast extract," *Bioresource technology,* vol. 114, pp. 518-522, 2012.

[38] H. Richter, M. E. Martin, and L. T. Angenent, "A two-stage continuous fermentation system for conversion of syngas into ethanol," *Energies,* vol. 6, pp. 3987-4000, 2013.

[39] M. T. Madigan, D. P. Clark, D. Stahl, and J. M. Martinko, *Brock Biology of Microorganisms 13th edition*: Benjamin Cummings, 2010.

[40] W. E. Balch, S. Schoberth, R. S. TANNER, and R. Wolfe, "Acetobacterium, a new genus of hydrogen-oxidizing, carbon dioxide-reducing, anaerobic bacteria," *International Journal of Systematic and Evolutionary Microbiology,* vol. 27, pp. 355-361, 1977.

[41] J. H. Sim, A. H. Kamaruddin, and W. S. Long, "Biocatalytic conversion of CO to acetic acid by Clostridium aceticum—Medium optimization using response surface methodology (RSM)," *Biochemical Engineering Journal,* vol. 40, pp. 337-347, 2008.

[42] T. D. Allen, M. E. Caldwell, P. A. Lawson, R. L. Huhnke, and R. S. Tanner, "Alkalibaculum bacchi gen. nov., sp. nov., a CO-oxidizing, ethanol-producing acetogen isolated from livestock-impacted soil," *International journal of systematic and evolutionary microbiology,* vol. 60, pp. 2483-2489, 2010.

[43] A. J. Grethlein, R. M. Worden, M. K. Jain, and R. Datta, "Evidence for production of n-butanol from carbon monoxide by Butyribacterium methylotrophicum," *Journal of fermentation and bioengineering,* vol. 72, pp. 58-60, 1991.

[44] J. Abrini, H. Naveau, and E.-J. Nyns, "Clostridium autoethanogenum, sp. nov., an anaerobic bacterium that produces ethanol from carbon monoxide," *Archives of microbiology,* vol. 161, pp. 345-351, 1994.

[45] J. S.-C. Liou, D. L. Balkwill, G. R. Drake, and R. S. Tanner, "Clostridium carboxidivorans sp. nov., a solvent-producing clostridium isolated from an agricultural settling lagoon, and reclassification of the acetogen Clostridium scatologenes strain

SL1 as Clostridium drakei sp. nov," *International journal of systematic and evolutionary microbiology,* vol. 55, pp. 2085-2091, 2005.

[46]   M. Köpke, C. Mihalcea, F. Liew, J. H. Tizard, M. S. Ali, J. J. Conolly*, et al.*, "2, 3-Butanediol production by acetogenic bacteria, an alternative route to chemical synthesis, using industrial waste gas," *Applied and environmental microbiology,* vol. 77, pp. 5467-5475, 2011.

[47]   S. N. Parshina, J. Sipma, Y. Nakashimada, A. M. Henstra, H. Smidt, A. M. Lysenko*, et al.*, "Desulfotomaculum carboxydivorans sp. nov., a novel sulfate-reducing bacterium capable of growth at 100% CO," *International Journal of Systematic and Evolutionary Microbiology,* vol. 55, pp. 2159-2165, 2005.

[48]   E. Pierce, G. Xie, R. D. Barabote, E. Saunders, C. S. Han, J. C. Detter*, et al.*, "The complete genome sequence of Moorella thermoacetica (f. Clostridium thermoaceticum)," *Environmental microbiology,* vol. 10, pp. 2550-2573, 2008.

[49]   M. D. Savage, Z. Wu, S. L. Daniel, L. L. Lundie, and H. L. Drake, "Carbon monoxide-dependent chemolithotrophic growth of Clostridium thermoautotrophicum," *Applied and environmental microbiology,* vol. 53, pp. 1902-1906, 1987.

[50]   T. V. Slepova, T. G. Sokolova, A. M. Lysenko, T. P. Tourova, T. V. Kolganova, O. V. Kamzolkina*, et al.*, "Carboxydocella sporoproducens sp. nov., a novel anaerobic CO-utilizing/H2-producing thermophilic bacterium from a Kamchatka hot spring," *International journal of systematic and evolutionary microbiology,* vol. 56, pp. 797-800, 2006.

[51]   S. S. Riggs and T. J. Heindel, "Measuring carbon monoxide gas—liquid mass transfer in a stirred tank reactor for syngas fermentation," *Biotechnology progress,* vol. 22, pp. 903-906, 2006.

[52]   J.-C. Charpentier, "Mass-transfer rates in gas-liquid absorbers and reactors," *Advances in chemical engineering,* vol. 11, pp. 1-133, 1981.

[53]   M. D. Bredwell and R. M. Worden, "Mass-transfer properties of microbubbles. 1. Experimental studies," *Biotechnology Progress,* vol. 14, pp. 31-38, 1998.

[54]   A. Fadavi and Y. Chisti, "Gas–liquid mass transfer in a novel forced circulation loop reactor," *Chemical Engineering Journal,* vol. 112, pp. 73-80, 2005.

[55]   W. T. Wu, J. Y. Wu, and J. Z. Jong, "Mass transfer in an airlift reactor with a net draft tube," *Biotechnology progress,* vol. 8, pp. 465-468, 1992.

[56]   J. Saxena and R. S. Tanner, "Effect of trace metals on ethanol production from synthesis gas by the ethanologenic acetogen, Clostridiumragsdalei," *Journal of industrial microbiology & biotechnology,* vol. 38, pp. 513-521, 2011.

[57]   M. Mohammadi, G. D. Najafpour, H. Younesi, P. Lahijani, M. H. Uzir, and A. R. Mohamed, "Bioconversion of synthesis gas to second generation biofuels: a review," *Renewable and Sustainable Energy Reviews,* vol. 15, pp. 4255-4273, 2011.

[58]   J. L. Gaddy and E. C. Clausen, "Clostridiumm ljungdahlii, an anaerobic ethanol and acetate producing microorganism," ed: Google Patents, 1992.

[59]   J. L. Cotter, M. S. Chinn, and A. M. Grunden, "Ethanol and acetate production by Clostridium ljungdahlii and Clostridium autoethanogenum using resting cells," *Bioprocess and biosystems engineering,* vol. 32, pp. 369-380, 2009.

[60] P. Maddipati, H. K. Atiyeh, D. D. Bellmer, and R. L. Huhnke, "Ethanol production from syngas by Clostridium strain P11 using corn steep liquor as a nutrient replacement to yeast extract," *Bioresource technology,* vol. 102, pp. 6494-6501, 2011.

[61] H. Younesi, G. Najafpour, and A. R. Mohamed, "Liquid fuel production from synthesis gas via fermentation process in a continuous tank bioreactor (CSTBR) using Clostridium ljungdahlii," *Iran J Biotechnol,* vol. 4, pp. 45-53, 2006.

[62] D. Xu, D. R. Tree, and R. S. Lewis, "The effects of syngas impurities on syngas fermentation to liquid fuels," *Biomass and Bioenergy,* vol. 35, pp. 2690-2696, 7// 2011.

[63] A. Ahmed, B. G. Cateni, R. L. Huhnke, and R. S. Lewis, "Effects of biomass-generated producer gas constituents on cell growth, product distribution and hydrogenase activity of Clostridium carboxidivorans P7T," *Biomass and Bioenergy,* vol. 30, pp. 665-672, 7// 2006.

[64] Metcalf, Eddy, F. L. Burton, H. D. Stensel, and G. Tchobanoglous, *Wastewater engineering: treatment and reuse*: McGraw Hill, 2003.

[65] F. Garcia-Ochoa and E. Gomez, "Bioreactor scale-up and oxygen transfer rate in microbial processes: an overview," *Biotechnology advances,* vol. 27, pp. 153-176, 2009.

[66] R. Sander, "Compilation of Henry's law constants (version 4.0) for water as solvent," *Atmospheric Chemistry & Physics,* vol. 15, 2015.

[67] APHA-AWWA-WEF, *Standard methods for the examination of water and wastewater*, 19th ed. American Public Health Association, 1015 Fifteenth Street, NW Washington, DC 20005: American Public Health Association/ American Water Works Association / Water Environment Federation, 1995.

[68] F. J. Baumann, "Dichromate reflux chemical oxygen demand. Proposed method for chloride correction in highly saline wastes," *Analytical Chemistry,* vol. 46, pp. 1336-1338, 1974.

[69] F. Pohland and D. Bloodgood, "Laboratory studies on mesophilic and thermophilic anaerobic sludge digestion," *Journal (Water Pollution Control Federation),* pp. 11-42, 1963.

[70] J. Bertsch and V. Müller, "Bioenergetic constraints for conversion of syngas to biofuels in acetogenic bacteria," *Biotechnology for biofuels,* vol. 8, p. 210, 2015.

[71] P. McCarty, "Energetics and bacterial growth. Faust, J., and Hunter, JV, editors: Organic Compounds in Aquatic Environments," ed: Marcel Dekker, Inc., New York, NY, 1971.

[72] E. R. Bruce and L. M. Perry, "Environmental biotechnology: principles and applications," *New York: McGrawHill,* vol. 400, 2001.

[73] A. W. Frankman, "Redox, pressure and mass transfer effects on syngas fermentation," 2009.

[74] H. Atiyeh and R. Huhnke, "Effects of Various Reducing Agents on Syngas Fermentation by "Clostridium ragsdalei"."

[75] S. Haus, S. Jabbari, T. Millat, H. Janssen, R.-J. Fischer, H. Bahl*, et al.*, "A systems biology approach to investigate the effect of pH-induced gene regulation on solvent production by Clostridium acetobutylicum in continuous culture," *BMC systems biology,* vol. 5, p. 10, 2011.

[76]   M. Mohammadi, H. Younesi, G. Najafpour, and A. R. Mohamed, "Sustainable ethanol fermentation from synthesis gas by Clostridium ljungdahlii in a continuous stirred tank bioreactor," *Journal of Chemical Technology and Biotechnology,* vol. 87, pp. 837-843, 2012.

[77]   S. Y. Lee, J. H. Park, S. H. Jang, L. K. Nielsen, J. Kim, and K. S. Jung, "Fermentative butanol production by Clostridia," *Biotechnology and bioengineering,* vol. 101, pp. 209-228, 2008.

[78]   K. Klasson, M. Ackerson, E. Clausen, and J. Gaddy, "Bioreactor design for synthesis gas fermentations," *Fuel,* vol. 70, pp. 605-614, 1991.

[79]   R. D. Tyagi, J. F. Blais, N. Meunier, and H. Benmoussa, "Simultaneous sewage sludge digestion and metal leaching—Effect of sludge solids concentration," *Water Research,* vol. 31, pp. 105-118, 1997/01/01 1997.

[80]   I. B. Technology, in *Sodium Bicarbonate Chemistry*, ed. 2931 Moose Trail, Elkhart, IN 46514 USA: Integrated Biomedical Technology, 2003.

[81]   A. P. H. Association, "Standard Methods for the Examination of Water and Wastewater," ed, 1995.

[82]   N. T. Eriksen and J. J. L. Iversen, "Determination of the overall volumetric mass transfer coefficient kLa, by a temperature dependent change of gas solubility," *Biotechnology techniques,* vol. 8, pp. 435-440, 1994.

[83]   P. Painmanakul, J. Wachirasak, M. Jamnongwong, G. Hébrard, P. Praserthdam, E. Editor*, et al.*, "Theoretical prediction of volumetric mass transfer coefficient (kLa) for designing an aeration tank," *Engineering Journal,* vol. 13, 2009.

[84]   V. Baranenko and V. Kirov, "Solubility of hydrogen in water in a broad temperature and pressure range," *Atomic Energy,* vol. 66, pp. 30-34, 1989.

[85]   M. Boudart and H. Hwang, "Solubility of hydrogen in small particles of palladium," *Journal of catalysis,* vol. 39, pp. 44-52, 1975.

[86]   A. Sharpe, "Solubility Explained," *Education in Chemistry,* vol. 1, p. 75, 1964.

Appendix A: Stoichiometric reactions of product formation

Stoichiometric reactions for acetic acid			
		Reactions	ΔG^o (kJ/e^-eq)
1	R_a	$\frac{1}{4}CO_2 + H^+ + e^- \rightarrow \frac{1}{8}CH_3COOH + \frac{1}{4}H_2O$	30.19
	R_d	$\frac{1}{2}CO + \frac{1}{2}H_2O \rightarrow \frac{1}{2}CO_2 + H^+ + e^-$	-49.88
	$R_{overall}$	$\frac{1}{2}CO + \frac{1}{4}H_2O \rightarrow \frac{1}{8}CH_3COOH + \frac{1}{4}CO_2$ $4CO + 2H_2O \rightarrow CH_3COOH + 2CO_2$	-19.67 -157.36
2	R_a	$\frac{1}{4}CO_2 + H^+ + e^- \rightarrow \frac{1}{8}CH_3COOH + \frac{1}{4}H_2O$	30.19
	R_d	$\frac{1}{2}H_2 \rightarrow H^+ + e^-$	-39.87
	$R_{overall}$	$\frac{1}{4}CO_2 + \frac{1}{2}H_2 \rightarrow \frac{1}{8}CH_3COOH + \frac{1}{4}H_2O$ $2CO_2 + 4H_2 \rightarrow CH_3COOH + 2H_2O$	-9.68 -77.44
Stoichiometric reactions for Ethanol			
		Reactions	ΔG^o (kJ/e^-eq)
3	R_a	$\frac{1}{6}CO_2 + H^+ + e^- \rightarrow \frac{1}{12}CH_3CH_2OH + \frac{1}{4}H_2O$	31.16
	R_d	$\frac{1}{2}CO + \frac{1}{2}H_2O \rightarrow \frac{1}{2}CO_2 + H^+ + e^-$	-49.88
	$R_{overall}$	$\frac{1}{2}CO + \frac{1}{4}H_2O \rightarrow \frac{1}{12}CH_3CH_2OH + \frac{1}{3}CO_2$ $6CO + 3H_2O \rightarrow CH_3CH_2OH + 4CO_2$	-18.72 -224.64
4	R_a	$\frac{1}{6}CO_2 + H^+ + e^- \rightarrow \frac{1}{12}CH_3CH_2OH + \frac{1}{4}H_2O$	31.16
	R_d	$\frac{1}{2}H_2 \rightarrow H^+ + e^-$	-39.87
	$R_{overall}$	$\frac{1}{6}CO_2 + \frac{1}{2}H_2 \rightarrow \frac{1}{12}CH_3CH_2OH + \frac{1}{4}H_2O$ $2CO_2 + 6H_2 \rightarrow CH_3CH_2OH + 3H_2O$	-8.71 -104.52

Appendix B: Hydrogen Seal Test

Background

Syngas fermentation is a microbial process, used to convert syngas into different sustainable biofuels and chemicals, such as ethanol and acetic acid etc. The digested food waste obtained from IATA *(Indre Agder og Telemark Avfallsselskap)* and *HRA (Hadeland og Ringerike Avfallsselskap AS)* were used as inoculum. Hydrogen and sodium bicarbonate as carbon source were introduced as gases substrate to produce acetic acid and ethanol. Inoculum contains microorganisms that started to consume hydrogen, subsequently, the pressure drop was experienced. The main objective of this master dissertation is to understand the overall syngas fermentation process, focusing on mass transfer phenomena, bacterial consumption of the provided substrates and products distribution.

Experimental setup

Before the project experiment start, there is a need to ensure whether pressure gauge working accurately or not and fermenter vessel sealed completely or not. That is why water is used as inoculum and hydrogen as syngas to pressurise the fermentation bioreactor. The bioreactor was equipped with a precision digital pressure gauge (CGH 1500), shown in Figure 1. The bioreactor has six valves, three of them were used. The injection valve was used for injection of hydrogen into the bioreactor, and flush out valve for flushing the air in order to achieve anaerobic condition and the effluent valve for taking a sample. Finally, measurement of pressure created by hydrogen gas injection was recorded at each 10-minute intervals.
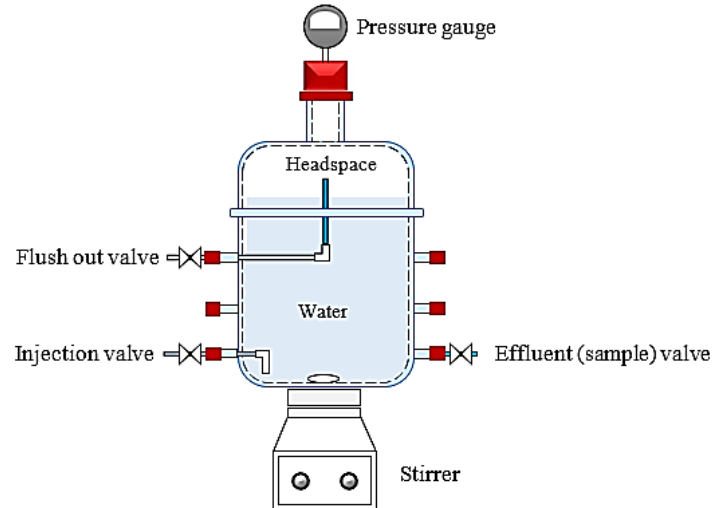
Figure 1: Schematic diagram of bioreactor with precision digital pressure gauge.

Method to hydrogen seal test

To expedite hydrogen seal test of the bioreactor. Initially, all the valves were fastened tightly, the test was conducted inside the fume hood chamber. Then, 3.25 L water was poured into the 4.132 L fermenter vessel (i.e. 882 mL headspace, shown in Figure 1) and stirred continuously at atmospheric temperature. Then, hydrogen gas was introduced through injection valve until the pressure reached 0.33 bar for the first time and started to measure headspace pressure with

respect to time (10-minute interval). The bioreactor was again pressurised at 0.56 bar and 1.04 bar.

Figure 2 shows the headspace pressure changes over time. Initially, pressure was noticed decreasing gradually from 0.33 bar to 0.29 bar within twenty-one hours, and then remained steady state. Then, couple times the bioreactor was pressurized at 0.56 and 1.04 bar headspace pressure after 142 and 262 hours of test experiment, respectively.
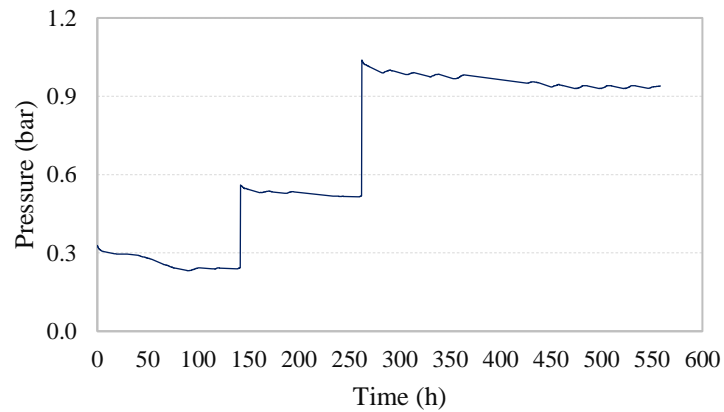
Figure 2: Headspace pressure during the experiment.

Key point: The headspace pressure was noticed decreasing and reached a steady state condition at the later stages of experiment. It implies that there was no any leakage in the bioreactor.

Drop in pressure due to dissolve of hydrogen in water at rate of about 0.00160 g/kg at 20°C and 1 atmospheric pressure. No headspace pressure drop was noticed after 558 hours later, as shown in Figure 2. This is because of enough dissolve of hydrogen in water (reached at a level of saturation point).

Appendix C: Sodium bicarbonate calculation

1 mole of carbon	22.4 L
Headspace volume	0.88 L
Molecular wt. of sodium bicarbonate	84 g/mole

0.88 L of headspace volume required $\dfrac{0.88}{22.4}$ mole of carbon

0.04 mole of carbon

Amount of required sodium bicarbonate   0.04 mole of carbon x 84 g/mole

3.31 g = 3.4 g

Appendix D: Mass balance in microbial growth

Total working volume (L)	3.25 L (inoculum)
Universal gas constant (R)	0.0821 atmL/molK
Average temperature	296 K
Acetic acid COD (undissociated organic)	1.07 gCOD/g compound
Hydrogen COD (undissociated organic)	8 gCOD/g compound
Molecular wt. of acetic acid	60 g/mol
Molecular wt. of hydrogen	1 g/mol

Total consumed hydrogen COD ($COD_{Hydrogen}$) calculation

Experimental data of hydrogen consumption

Duration (h)	No. of injection	Injected headspace pressure	Decreased headspace pressure	Consumed hydrogen			
		(a) (bar)	(b) (bar)	(a-b) (bar)	(a-b) (atm)	(mmol/L)	(mmol)
0-71	1	0.283	0.219	0.064	0.063	2.599	8.447
71-313	2	1.010	0.712	0.298	0.294	12.102	39.331
313-407	3	1.000	-0.201	1.201	1.185	48.773	158.513
407-478	4	1.002	-0.118	1.120	1.105	45.484	147.822
478-527	5	1.115	-0.379	1.494	1.474	60.672	197.184
527-577	6	1.033	-0.185	1.218	1.202	49.464	160.757
577-646	7	1.001	-0.398	1.399	1.381	56.814	184.646
646-694	8	1.005	-0.060	1.065	1.051	43.250	140.563
694-744	9	1.000	0.085	0.915	0.903	37.159	120.765
744-839	10	1.012	0.310	0.702	0.693	28.509	92.653
839-1174	11	1.023	0.171	0.852	0.841	34.600	112.450
1174-1297	12	1.511	1.411	0.100	0.099	4.061	13.198
Total		11.995	1.567	10.428	10.291	423.486	1376.630

Note: Decreased headspace pressure represents the decrease of headspace pressure due to the consumption of hydrogen by the microorganisms (dissolved hydrogen in the inoculum).

Total consumed hydrogen	1377 mmol = 1.377 mol
Total consumed hydrogen COD ($COD_{Hydrogen}$)	1.377 (mol) x 1 (g/mol) x 8 (gCOD/g)
	11.02 gCOD

Total produced acetic acid COD ($COD_{Acetic\ acid}$) calculation

Experimental data of acetic acid and other organic acids production

Time (h)	Acetic acid (mmol/L)	Propionic acid (mmol/L)	Isobutyric acid (mmol/L)	Butyaric acid (mmol/L)	Isovaleric acid (mmol/L)
Start	31.56	2.98	0.55	0.00	0.65
48	31.85	3.13	0.54	0.76	0.00
264	32.19	3.75	0.98	0.00	1.36
312	34.33	4.05	0.97	0.28	1.36
408	40.75	3.87	0.79	0.23	1.06
553	51.87	4.22	0.99	0.28	1.38
745	61.93	4.41	1.02	0.33	1.46
912	60.99	4.16	0.92	0.00	1.33
1080	65.20	4.14	0.97	0.30	1.40
1176	67.70	4.22	0.95	0.32	1.35
1297	67.55	4.59	1.10	0.00	1.54

Total acetic acid production	67.55 – 31.56 mmol/L
	35.99 mmol/L
	35.99 (mmol/L) x 3.25 (L)
	$\dfrac{35.99 \times 3.25}{1000}$ mol
	0.117 mol

Total produced acetic acid COD ($COD_{Acetic\ acid}$)	0.1177(mol) x 60(g/mol) x 1.07(gCOD/g)
	7.51 gCOD

Others organic acid COD were not calculated because of being small amount.

Total produced inoculum COD (COD_{Inoculum}) calculation

Experimental data of COD_T and COD_S production.

Time (h)	COD_T_in (g/L)	COD_S_in (g/L)	COD_T_out (g/L)	COD_S_out (g/L)
Start	11.76	6.90	-	-
48	-	-	13.18	6.46
264	-	-	11.40	6.44
312	-	-	12.52	6.70
408	-	-	11.96	7.24
553	-	-	12.64	8.28
745	-	-	14.44	9.34
912	-	-	13.24	7.76
1080	-	-	14.60	8.86
1176	-	-	15.40	8.94
1297			15.28	9.12

Total produced inoculum (COD_{Inoculum})	15.28 – 11.76 (gCOD/L)
	3.52 (gCOD/L)
	3.52 (gCOD/L) x 3.25 (L)
	11.44 gCOD

Total produced inoculum COD (COD_{Inoculum})	11.44 gCOD

Summary:

Total consumed hydrogen COD (COD_{Hydrogen})	11.02 gCOD
Total produced acetic acid COD (COD_{Acetic acid})	7.51 gCOD
Total produced inoculum COD (COD_{Inoculum})	11.44 gCOD

Appendix E: Solubility of hydrogen in the inoculum

Total working volume (L)	3.25 L (inoculum)
Average temperature	296 K
Universal gas constant (R)	0.0821 atmL/molK
Henry's constant for hydrogen (k_{H,H_2})	7.8 10^{-4} mol/atmL

Henry's law

$$C_H = k_{H,H_2} P_{Gas}$$

where C_H is the solubility of hydrogen in the inoculum (mol/L), k_{H,H_2} is Henry's coefficient (mol/atmL), and P_{Gas} is the headpsace partial pressure of gas (atm).

Duration (h)	Injected headspace pressure (a) (bar)	Decreased headspace pressure (b) (bar)	Headspace partial pressure (P_{Gas})		Solubility (C_H)
			(a-b) (bar)	(a-b) (atm)	(mol/L)
0-71	0.283	0.219	0.064	0.063	0.000049
71-313	1.010	0.712	0.298	0.294	0.000229
313-407	1.000	-0.201	1.201	1.185	0.000925
407-478	1.002	-0.118	1.120	1.105	0.000862
478-527	1.115	-0.379	1.494	1.474	0.001150
527-577	1.033	-0.185	1.218	1.202	0.000938
577-646	1.001	-0.398	1.399	1.381	0.001077
646-694	1.005	-0.060	1.065	1.051	0.000820
694-744	1.000	0.085	0.915	0.903	0.000705
744-839	1.012	0.310	0.702	0.693	0.000541
839-1174	1.023	0.171	0.852	0.841	0.000656
1174-1297	1.511	1.411	0.100	0.099	0.000077
Total	11.995	1.567	10.428	10.291	0.008029

Note: Decreased headspace pressure represents the decrease of headspace pressure due to the consumption of hydrogen by the microorganisms (dissolved hydrogen in the inoculum).

Appendix F: Stoichiometry reaction and biomass yield

Reaction	ΔG_C^o (kJ/e^-eq)
$\frac{1}{5}CO_2 + \frac{1}{10}HCO_3^- + H^+ + e^- \rightarrow \frac{1}{10}CH_3COCOO^- + \frac{2}{5}H_2O$ (Pyruvate)	35.09
$\frac{1}{2}H_2 \rightarrow H^+ + e^-$ (Hydrogen as electron donor)	-39.87

Using following formula (Taken from book, Energetics and bacterial growth).

$$\Delta G_P = 35.09 - \Delta G_C^o \qquad \text{(Eq. 1)}$$

$$\Delta G_S = \frac{\Delta G_P}{\varepsilon^n} + \frac{\Delta G_{PC}}{\varepsilon} \qquad \text{(Eq. 2)}$$

where, ΔG_S = free energy to convert one electron equivalent (e^- eq) of the carbon source to cell material

ΔG_P = free energy to convert e^- eq of the carbon source to the pyruvate intermediate

ε = energy transfer efficiency

n = +1 if ΔG_s is positive and -1 if energy is produced

ΔG_{PC} = free energy per e^- eq of cells to reduce nitrogen to ammonia

ΔG_C^o = free energy per e^- eq of electron donor

Free energy to convert e^- eq of carbon source to the pyruvate intermediate (using equation 1).

ΔG_P (H_2 as an electron donor)	74.96 kJ/e^-eq

$$\varepsilon\Delta G_r\left(\frac{f_e}{f_S}\right) = -\frac{\Delta G_P}{\varepsilon^n} + \frac{\Delta G_{PC}}{\varepsilon} \qquad \text{(Eq. 3)}$$

$$f_e + f_S = 1 \qquad \text{(Eq. 4)}$$

Where, ΔG_r = free energy released per e^- eq of donor oxidised for energy generation.

f_e = e^- mole of substrate oxidized per e^- mole of substrate used

f_S = e- mole of substrate used for cell synthesis per e- mole of substrate used

And,

The pyruvate carbon is converted to cellular carbon. The energy required, ΔG_{PC} is based on an estimated value of 3.33 kJ/g cells (taken from book, Energetics and bacterial growth). An

electron equivalent cell is $113/20 = 5.56$ g when NH_4^+ is used as nitrogen source and $\Delta G_{PC} = 3.33$ x $5.56 = 18.8$ kJ/e^-eq. Similarly, for NO_3^- as nitrogen source, electron equivalent cell is $113/28$ $= 4.04$ gm and $\Delta G_{PC} = 3.33$ x $4.04 = 13.5$ kJ/e^-eq.

Biomass yield, associated stoichiometrically with ethanol formation.

$\varepsilon = 0.6$ (assume)

$\Delta G_P = 35.09 - (-39.87) = 74.96$ kJ/e^-eq (H_2 is an electron donor)

$\Delta G_r = 30.19 - 39.87 = -9.68$ kJ/e^-eq

Since ΔG_P is positive, $n = +1$. ΔG_{PC} is 18.8 kJ/e^-eq when NH_4^+ is used as nitrogen source for cell synthesis. Hence,

$$\Delta G_S = \frac{74.96}{0.6^1} + \frac{18.8}{0.6} = 156.27 \, \text{kJ/}e^-\text{eq}$$

Determine f_e and f_S using 2.3.

$$0.6 \text{x}(-9.68)\text{x}\left(\frac{f_e}{f_S}\right) = -156.27$$

$$f_e = 26.91 f_S$$

$$f_S + 26.91 f_S = 1$$

$$f_S = 0.036 \, \frac{\text{g cellCOD}}{\text{g COD used}}$$

$$f_e = 0.964$$

Determine the yield based on COD. For biomass $C_5H_7O_2N$, for 1 g cells $= 1.42$ g COD. Hence, the yield is

$$Y = \left(\frac{0.036 \text{ gCOD/gCOD}}{1.42 \text{ gCOD/gVSS}}\right) = 0.025 \text{ gVSS/gCOD}$$

Using the same procedure above applied, the biomass yields with energy capture efficiency ranged from 0.1 to 1 have been calculated as follows.

Energy capture efficiency (ε)									
0.1	0.2	0.3	0.4	0.5	0.6	0.7	0.8	0.9	1
0.00073	0.0029	0.00648	0.01144	0.01772	0.02524	0.03391	0.04365	0.05435	0.0659

Biomass yield, associated stoichiometrically with ethanol formation.

$= 0.6$ (assume)

$\Delta G_P = 35.09 - (-39.87) = 74.96 \, 74.96$ kJ/e^-eq (H_2 is an electron donor)

$\Delta G_r = 31.16 - 39.87 = -8.71$ kJ/e^-eq

Since ΔG_P is positive, $n = +1$. ΔG_{PC} is 18.8 kJ/e^-eq when NH_4^+ is used as nitrogen source for cell synthesis. Hence,

$$\Delta G_S = \frac{74.96}{0.6^1} + \frac{18.8}{0.6} = 156.27 \, \text{kJ/}e^-\text{eq}$$

Determine f_e and f_S using 2.3.

$$0.6 \times (-8.71) \times \left(\frac{f_e}{f_S} \right) = -156.27$$

$$f_e = 29.91 f_S$$

$$f_S + 29.91 f_S = 1$$

$$f_S = 0.032 \, \frac{\text{g cellCOD}}{\text{g COD used}}$$

$$f_e = 0.968$$

Determine the yield based on COD. For biomass $C_5H_7O_2N$, for 1 g cells = 1.42 g COD. Hence, the yield is

$$Y = \left(\frac{0.032 \, \text{gCOD/gCOD}}{1.42 \, \text{gCOD/gVSS}} \right) = 0.0227 \, \text{gVSS/gCOD}$$

Using the same procedure above applied, the biomass yields with energy capture efficiency ranged from 0.1 to 1 have been calculated as follows.

Energy capture efficiency (ε)									
0.1	0.2	0.3	0.4	0.5	0.6	0.7	0.8	0.9	1
0.00065	0.00261	0.00584	0.01031	0.01598	0.02279	0.03066	0.03952	0.04928	0.05986

Stoichiometry of Biological Reactions

$$R = f_e R_a + f_S R_{CS} - R_d \qquad \text{(Eq. 5)}$$

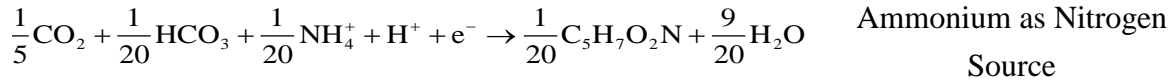Where, R = overall balanced reaction

R_a = half reaction for electron accepter

R_{CS} = half reaction for synthesis of cell tissue
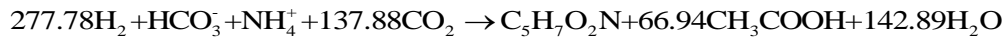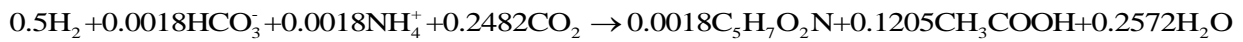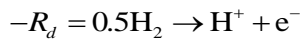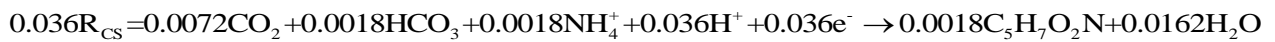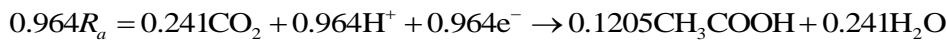
R_d = half reaction for electron donor

f_e = fraction of electron donor used for energy

f_S = fraction of electron donor used for cell synthesis

Cell synthesis equations (R_{CS})

$\frac{1}{5}CO_2+\frac{1}{20}HCO_3^-+\frac{1}{20}NH_4^++H^++e^- \rightarrow \frac{1}{20}C_5H_7O_2N+\frac{9}{20}H_2O$	Ammonium as Nitrogen Source

Determine the balanced stoichiometric reaction for acetic acid formation with biomass yields, using equation 5.

Stoichiometric reactions for acetic acid with biomass yields	
R_a	$\frac{1}{4}CO_2+H^++e^- \rightarrow \frac{1}{8}CH_3COOH+\frac{1}{4}H_2O$
R_d	$\frac{1}{2}H_2 \rightarrow H^++e^-$

$0.964R_a=0.241CO_2+0.964H^++0.964e^- \rightarrow 0.1205CH_3COOH+0.241H_2O$

$0.036R_{CS}=0.0072CO_2+0.0018HCO_3^-+0.0018NH_4^++0.036H^++0.036e^- \rightarrow 0.0018C_5H_7O_2N+0.0162H_2O$

$-R_d=0.5H_2 \rightarrow H^++e^-$

$0.5H_2+0.0018HCO_3^-+0.0018NH_4^++0.2482CO_2 \rightarrow 0.0018C_5H_7O_2N+0.1205CH_3COOH+0.2572H_2O$

$277.78H_2+HCO_3^-+NH_4^++137.88CO_2 \rightarrow C_5H_7O_2N+66.94CH_3COOH+142.89H_2O$

Determine the stoichiometric reaction for ethanol formation with biomass yields, using equation 5.

Stoichiometric reactions for Ethanol formation with biomass yields	
R_a	$\frac{1}{6}CO_2+H^++e^- \rightarrow \frac{1}{12}CH_3CH_2O+\frac{1}{4}H_2O$
R_d	$\frac{1}{2}H_2 \rightarrow H^++e^-$

$0.968R_a=0.161CO_2+0.968H^++0.968e^- \rightarrow 0.0806CH_3CH_2OH+0.242H_2O$

$0.032R_{CS}=0.0064CO_2+0.0016HCO_3^-+0.0016NH_4^++0.032H^++0.032e^- \rightarrow 0.0016C_5H_7O_2N+0.0144H_2O$

$-R_d=0.5H_2 \rightarrow H^++e^-$

$0.5H_2+0.0016HCO_3^-+0.0016NH_4^++0.1674CO_2 \rightarrow 0.0016C_5H_7O_2N+0.0806CH_3CH_2OH+0.2564H_2O$

$312.5H_2+HCO_3^-+NH_4^++104.63CO_2 \rightarrow C_5H_7O_2N+50.38CH_3COOH+160.25H_2O$